Athens Journal of Technology & Engineering

Quarterly Academic Periodical, Volume 9, Issue 4, December 2022
URL: https://www.athensjournals.gr/ajte
Email: journals@atiner.gr
e-ISSN: 2241-8237 DOI: 10.30958/ajte

Athens Journal of Technology & Engineering

Published by the Athens Institute for Education and Research (ATINER)

****
*

ATINER is an Athens-based World Association of Academics and Researchers based in Athens. ATINER is an independent and non-profit Association with a Mission to become a forum where Academics and Researchers from all over the world can meet in Athens, exchange ideas on their research and discuss future developments in their disciplines, as well as engage with professionals from other fields. Athens was chosen because of its long history of academic gatherings, which go back thousands of years to Plato's Academy and Aristotle's Lyceum. Both these historic places are within walking distance from ATINER's downtown offices. Since antiquity, Athens was an open city. In the words of Pericles, Athens"…is open to the world, we never expel a foreigner from learning or seeing". ("Pericles' Funeral Oration", in Thucydides, The History of the Peloponnesian War). It is ATINER's mission to revive the glory of Ancient Athens by inviting the World Academic Community to the city, to learn from each other in an environment of freedom and respect for other people's opinions and beliefs. After all, the free expression of one's opinion formed the basis for the development of democracy, and Athens was its cradle. As it turned out, the Golden Age of Athens was in fact, the Golden Age of the Western Civilization. Education and (Re)searching for the 'truth' are the pillars of any free (democratic) society. This is the reason why Education and Research are the two core words in ATINER's name.

****

The ***Athens Journal of Technology & Engineering (AJTE)*** is an Open Access quarterly double-blind peer reviewed journal and considers papers from all areas engineering (civil, electrical, mechanical, industrial, computer, transportation etc), technology, innovation, new methods of production and management, and industrial organization. Many of the papers published in this journal have been presented at the various conferences sponsored by the Engineering & Architecture Division of the Athens Institute for Education and Research (ATINER). All papers are subject to ATINER's Publication Ethical Policy and Statement.

The Athens Journal of Technology & Engineering
ISSN NUMBER: 2241-8237- DOI: 10.30958/ajte
Volume 9, Issue 4, December 2022
Download the entire issue (PDF)

Athens Journal of Technology & Engineering
Editorial and Reviewers' Board

President's Message

All ATINER's publications including its e-journals are open access without any costs (submission, processing, publishing, open access paid by authors, open access paid by readers etc.) and is independent of presentations at any of the many small events (conferences, symposiums, forums, colloquiums, courses, roundtable discussions) organized by ATINER throughout the year and entail significant costs of participating. The intellectual property rights of the submitting papers remain with the author. Before you submit, please make sure your paper meets the basic academic standards, which includes proper English. Some articles will be selected from the numerous papers that have been presented at the various annual international academic conferences organized by the different divisions and units of the Athens Institute for Education and Research. The plethora of papers presented every year will enable the editorial board of each journal to select the best, and in so doing produce a top-quality academic journal. In addition to papers presented, ATINER will encourage the independent submission of papers to be evaluated for publication.

The current issue is the fourth of the ninth volume of the *Athens Journal of Technology & Engineering (AJTE),* published by the Engineering & Architecture Division of ATINER.

Gregory T. Papanikos, President, ATINER.

Athens Institute for Education and Research
A World Association of Academics and Researchers

13th Annual International Conference on Civil Engineering
19-22 June 2023, Athens, Greece

The Civil Engineering Unit of ATINER is organizing its **13th Annual International Conference on Civil Engineering, 19-23 June 2023, Athens, Greece** sponsored by the Athens Journal of Technology & Engineering. The aim of the conference is to bring together academics and researchers of all areas of Civil Engineering other related areas. You may participate as stream leader, presenter of one paper, chair of a session or observer. Please submit a proposal using the form available (https://www.atiner.gr/2023/FORM-CIV.doc).

Academic Members Responsible for the Conference

- **Dr. Dimitrios Goulias**, Head, Civil Engineering Unit, ATINER and Associate Professor & Director of Undergraduate Studies Civil & Environmental Engineering Department, University of Maryland, USA.

Important Dates

- Abstract Submission: **21 March 2023**
- Acceptance of Abstract: 4 Weeks after Submission
- Submission of Paper: **22 May 2023**

Social and Educational Program

The Social Program Emphasizes the Educational Aspect of the Academic Meetings of Atiner.

- Greek Night Entertainment (This is the official dinner of the conference)
- Athens Sightseeing: Old and New-An Educational Urban Walk
- Social Dinner
- Mycenae Visit
- Exploration of the Aegean Islands
- Delphi Visit
- Ancient Corinth and Cape Sounion

Conference Fees

Conference fees vary from 400€ to 2000€
Details can be found at: https://www.atiner.gr/fees

Athens Institute for Education and Research
A World Association of Academics and Researchers

11th Annual International Conference on Industrial, Systems and Design Engineering, 19-22 June 2023, Athens, Greece

The Industrial Engineering Unit of ATINER will hold its **11th Annual International Conference on Industrial, Systems and Design Engineering, 19-23 June 2023, Athens, Greece** sponsored by the Athens Journal of Technology & Engineering.The aim of the conference is to bring together academics, researchers and professionals in areas of Industrial, Systems, Design Engineering and related subjects. You may participate as stream leader, presenter of one paper, chair of a session or observer. Please submit a proposal using the form available (https://www.atiner.gr/2023/FORM-IND.doc).

Important Dates

- Abstract Submission: **21 March 2023**
- Acceptance of Abstract: 4 Weeks after Submission
- Submission of Paper: **22 May 2023**

Academic Member Responsible for the Conference

- **Dr. Theodore Trafalis**, Director, Engineering & Architecture Division, ATINER, Professor of Industrial & Systems Engineering and Director, Optimization & Intelligent Systems Laboratory, The University of Oklahoma, USA.

Social and Educational Program

The Social Program Emphasizes the Educational Aspect of the Academic Meetings of Atiner.

- Greek Night Entertainment (This is the official dinner of the conference)
- Athens Sightseeing: Old and New-An Educational Urban Walk
- Social Dinner
- Mycenae Visit
- Exploration of the Aegean Islands
- Delphi Visit
- Ancient Corinth and Cape Sounion

More information can be found here: https://www.atiner.gr/social-program

Conference Fees

Conference fees vary from 400€ to 2000€

Details can be found at: https://www.atiner.gr/fees

Athens Journal of Technology and Engineering - Volume 9, Issue 4, December 2022 – Pages 267-280

Dependency Visualization Tool for Decision Support Systems with Preferential Dependencies

By Sobitha Samaranayake & Shehan Senanayake±*

Large-scale and long-term projects often consist of subtasks linked to each other with certain dependencies that need to be completed. Dependency evaluation and visualization tools can help identify project bottlenecks, prioritize tasks, and plan resource allocation. Hence, visualization tools can improve the efficiency of project interdependency management by dynamically displaying the project constraints and task dependencies. Many of the dependency visualization tools that are being used in the industry are designed to manage internal dependencies and task dependencies. In this work, we introduce an online tool for creating and maintaining visualizations of logical dependencies and preferential dependencies. The proposed online tool can be used with any process that is defined in terms of completing a well-defined logical sequence of activities that must be completed in order to reach a specific target, such as project planning, or with any process that can be completed by different sequences of activities, such as college degree planning (due to elective courses) or interest-aligned career planning.

Keywords: *academic decision making, decision support system, data visualization, dependency visualization, project management*

Introduction

There are different types of decision support systems (DSSs), such as data-driven systems, knowledge-driven systems, and model-driven systems. Both data-driven and knowledge-driven systems use either a file system or a data warehouse to store data, and these systems use charts, maps, graphs, or other graphic tools to visualize data. Model-driven DSSs are created for special purpose decision support needs and they can help analyze different scenarios.

Model-driven DSSs are used for analyzing project planning and scheduling problems. Large-scale and long-term projects often consist of subtasks linked to each other with certain dependencies that need to be completed. There are different types of task dependencies, such as logical, constraint-based, or preferential dependencies.

Logical dependencies are the tasks of a project that are necessary for a project's completion. They are the output for all of the preceding tasks and may not run parallel with other tasks. Tasks may have multiple preceding tasks and multiple succeeding tasks. Predecessors must complete before successors can start so completing logical dependencies can be considered as a scheduling problem.

*Associate Professor, University of Wisconsin-Whitewater, USA.
±Graduate Student, University of Wisconsin-Whitewater, USA.

Many visualization tools are available for creating charts, maps, and graphs for logical dependencies. Program Evaluation and Review Technique (PERT) (Kerzner 2003) is a project management tool that is widely used to visualize the timeline and the work that must be done to complete a project. The critical path is the longest sequence of tasks that must be completed to complete a project. Gantt charts (Clark 1922) are used for calculating the critical path and showing tasks displayed against time, and hence they are commonly used for tracking the completion of logical dependencies.

Preferential dependencies occur when there are many possibilities for completing a sequence of tasks. There may be many options for completing a particular task and the choices for completing preceding tasks may influence the choices for succeeding tasks. Hence, choosing a particular path to complete a sequence of such task dependencies may depend on user preferences, such as cost, time, quality, or resource allocation.

Data visualization tools help decision makers to match their creativity and background knowledge with the enormous storage and processing capabilities of advanced computing systems. Using advanced visual interfaces, humans can interact directly with data analysis (Alves and Cota 2018). There is a dearth of visualization tools for systems with preferential dependencies, especially when there are many choices for each task. This paper will focus on developing visualization tools for systems with preferential dependencies. We will consider a generic model that can represent a range of systems where the goal is to select a subset of a list of tasks and then complete each task in that subset. After reviewing the scope of the current visualization tools, we present a visualization tool that is capable of visualizing a variety of preferential dependencies.

Literature Review

Decision support systems have been used for a wide variety of decision-making activities. Power (2008) investigated historic foundation of data-driven DSSs and reported that data-driven DSSs have been used for many decision-making activities, such as air-defense command and control, geographic information systems, customer relationship management systems, static and real-time performance monitoring, and executive information systems. DSSs help businesses in many different ways, such as generating more accurate projections, better inventory management, data analysis, sales optimization, and optimizing industry-specific systems (Trieu 2017, Power 2013, Feng 2016, Rouhani et al. 2018).

Web based DSSs adds a new dimension to the evolution of DSSs, and many of the information systems people interact with are powered by decision support systems. Wright et al. (2009) analyzed three case studies to evaluate the potential of creating and sharing clinical DSSs with Web 2.0 technologies. Sugumaran and Sugumaran (2007) analyzed the evolution of web-based spatial DSSs. Krishnaiyer and Chen (2017) explained an implementation of a web-based visual DSS that helped an organization to successfully turn around the scheduling and capacity planning function along with extending the success to customer service, and warehouse operations.

Knowledge-driven DSSs use facts, rules, and procedures to analyze data to help users make intelligent decisions. Hence, knowledge-driven educational DSS can provide valuable information to students, educators, and educational organizations, but developing an educational DSS is a complex process. Due to the flexibility of a credit system of education, degree requirements are different from organization to organization, hence, applying data mining techniques to educational data is challenging. Vo and Nguyen (2012) proposed a knowledge-driven educational decision support system for education with a semester credit system by taking advantage of educational data mining. Anardani et al. (2019) discussed the design of student performance monitoring information systems by applying the business intelligence concept. Moscoso-Zea et al. (2019) presented an infrastructure to analyze educational data and academic processes and for the creation of explicit knowledge using different algorithms and methods of educational data mining.

Model-driven DSSs are helpful for academic advisors to make more appropriate and reasonable decisions about student's studies and give further support to students for their course planning. There has been interest in designing a DSS for course planning. Siddiqui et al. (2018) introduced a web-based group DSS for academic term preparation at a business college of a large Middle Eastern university. Roushan et al. (2014) presented a DSS for course planning. Miranda et al. (2012) developed a web-based DSS for course and classroom scheduling. Oladokun and Oyewole (2015) presented a DSS for university admission seekers. Al-Qaheri et al. (2011) presented a DSS for a course scheduler. Meyer et al. (2021) presented an application of information technology in providing decision support in college planning.

Visual representation in DSSs has been discussed by many researchers. Basole et al. (2016) analyzed the effectiveness of using lists, matrices, and network visualization for business ecosystem analysis. Kuru et al. (2014) demonstrated the benefits of using machine learning algorithms and digital image processing techniques to build an intelligent diagnostic DSS in medical genetics. Hennocq et al. (2021) presented a literature review of all the methods for analyzing 2D pictures for diagnostic purposes. Interactive data visualization dashboards are being used for visualizing and analyzing trends in large volumes of data (Huber et al. 2018, West et al. 2015, Morgan et al. 2006, Nevo et al. 2015). Trase and Fink (2014) designed a model-driven visualization tool for use with model-based engineering projects. Burnay et al. (2019) analyzed some recent approaches of DSSs and information systems that present domain-specific and visualization-based user communication strategies and interfaces to support decision-making.

Overview of the Current Visualization Tools

Over the past couple of decades, there has been an interest in improving the efficiency of large projects that require the completion of multiple tasks in order to achieve the end goal. This has become its own process which is now done by people who work in positions such as project managers and academic advisors.

Although there are many different ways of presenting the information related to multiple tasks, such as using a text file to document the steps, the most efficient method of presenting such information is by using a visualization of the process.

We consider model-driven systems where the requirement is to complete a sequence of tasks. There are two main types of dependencies between tasks: logical dependencies and preferential dependencies. Having some sort of visualization makes the project planning or task scheduling more convenient as it is easier to read and understand certain dependencies between the tasks that make up the bigger project. Many visualization tools exist for systems where predecessors must complete before successors can start. Project management is such a system, and different visualizations such as flow charts, Unified Modeling Language (UML) diagrams, Program Evaluation and Review Technique (PERT) charts, and Gantt charts are used to visualize the required information. Flow charts and UML diagrams visualize the workflow and actions taken by the client of a specific project to help the team understand what features the product needs to support. Flow charts can display a process step by step. However, they focus on visualizing processes that require decision making based on how to do something instead of what to do. On the other hand, PERT charts visualize the step-by-step tasks that need to be completed by a team in order to complete the project. However, the PERT chart only displays sequential dependencies and concurrent dependencies. Also, the PERT chart does not display any sort of progress along the graph as it is a static graph once it is generated. This means the user has to keep track of where they are, or they will have to find their current task first and then look for the next step each time they refer to the visualization.

Similar to PERT charts, Gantt charts also visualize the tasks that need to be completed by a team. Gantt charts use a table format where the columns represent a time frame (days or months) and the rows represent the specific tasks. This allows the user to schedule tasks. An additional feature this provides is the ability to track the progress of each task as it shows a completed percentage. A disadvantage to using the Gantt chart is that it is not capable of showing dependencies between tasks as the tasks are usually displayed in each row, and the process is like a waterfall where you complete the top one and move on to the next. This makes processes such as academic advising very inconvenient as the path a student has to follow for a degree usually has classes with prerequisites.

Three main visualization systems that are currently used in the industry are Lucidchart (Faulkner 2018), Visio Data Visualizer (Parker 2016), and ProjectManager (tool provided by Projectmanager.com). Lucidchart is one of the most used tools in the industry right now as it allows a lot of functionality for all types of processes. However, the user has to create the visualizations using the drag and drop method and a list of built-in shapes. Using this technique, the user can create a static diagram with the information they want to display. Similarly, the Visio Data Visualizer allows the user to create a table in Excel and export it as a Visio diagram. This will generate a process diagram using the information from the table. Both Lucidchart and Visio do a great job at creating process diagrams similar to flowcharts, but they focus more on how to do something instead of what to do. Additionally, the visualization they create is static and the user cannot interact with it to track their progress. The tool from Projectmanager.com on the other hand is able to track user progress. This tool allows the user to import data from a CSV file as well and the user can drag and drop the initial visualization. However, it usually tracks the progress of each individual task instead of the overall process.

A dependency graph is a flow chart or a directed graph representing relationships between the nodes. There are several tools available for creating static dependency graphs. Sankey diagram is a graph that is used for visualizing a flow from one set of values to another. Lupton and Allwood (2017) presented a common data structure and a systematic method for generating different hybrid Sankey diagrams from a dataset. Oran et al. (2019) used Sankey diagrams to identify and visualize progress and mobility patterns in higher education. Horvath et al. (2018) used Sankey diagrams to visualize student flows to track retention and graduate rates. Designing a dependency visualization tool for systems with preferential dependencies is a complex process since the graph needs to be dynamically updated, based on the preferences. In this work, we introduce a visualization tool that is capable of visualizing a variety of preferential dependencies.

Method

Consider a model where the goal is to select a subset of a predefined list of tasks and then complete each task in that subset using the following requirements:

- Each task may consist of a set of subtasks such that a task can be completed by either type a: completing k subtasks from a set of p subtasks where $1 \leq k \leq p$, or type b: completing at least m subtasks, but no more than n subtasks from a set of p subtasks where $0 \leq m \leq n \leq p$, or completing a combination of type a and type b conditions.
- Predecessors must complete before successors
- Some of the subtasks are predecessors to multiple tasks.

There are many systems that can be modeled using the above requirements. None of the existing visualization tools are able to display the task dependencies described by the above model.

One of the goals of this work is to develop visualization tools to analyze the following questions for systems represented by the above model:

- What are the dependencies between the tasks?
- What is the current progress of the project?
- What are the next possible steps?

We answer these questions using a graph-based dependency visualization tool (DVT) which is implemented as a directed graph where the nodes represent a subset of tasks and the edges represent the dependencies.

We use a data model that incorporates a flexible grid system $G(N, D, O)$ to represent tasks and their dependencies as a directed graph where $N = \{N_1, N_2, \dots, N_n\}$ is a set of nodes, D is the dimension of the grid, and O is the orientation. Each node N_i is a task expressed using a tuple $N_i = (L, M, C, P, D, S, \delta)$ where L is the location of the node, M is a set of subtasks associated with the node, C is a logical condition on M that defines the rule for completion of a task, P is a set of predecessors, $, D$ is a logical condition that defines dependencies on preceding nodes, S is a set of successors, and $\delta: M \to \{1, 0\}$ is a function such that $\delta(M) = 1$ if M satisfies the logical condition C and $\delta(M) = 0$ otherwise. (This function is used to check if the task is complete). Nodes of the directed graph can be arranged vertically or horizontally. Our data model allows us to easily modify node locations and edges between the nodes.

To demonstrate the potential of the DVT, we will now look at a few example scenarios.

Implementation

College degree planning involves selecting a set of courses to fulfill degree requirements. Degree requirements are defined in terms of number of units or courses that needs to be completed. Many courses specify prerequisites or course dependencies.

There are more than 150 major emphasis areas offered at University of Wisconsin-Whitewater (UWW), and each of those emphasis areas is defined using a set of requirements. A typical requirement belongs to one of the following categories:

- Type A: complete k courses from a set of p courses where $1 \le k \le p$
- Type B: complete at least m courses/units, but no more than n courses/ units from a set of p courses where $0 \le m \le n \le p$
- Type C: complete k units from a set of p courses where $1 \le k \le p$
- Type D: combination of Type A, Type B, and/or Type C requirements

Figure 1 displays degree requirements for computer science major at UWW. Computer science students should complete three courses in software development fundamentals, five core courses, and twelve units of elective courses (four elective courses).

Many courses specify prerequisite relationships that are often defined using one of, all of, either or, and, or a combination of those logical relationships among a list of predefined courses. There may be prerequisites of prerequisite courses. Hence, a directed acyclic graph is the best structure to represent prerequisite relationships where nodes represent course lists and edges represent their dependencies.

Figure 1. *Degree Requirements for Computer Science Major at UWW*

Computer Science Requirements (BA/BS)

Major Requirements: [1]		
Software Development Fundamentals:		
COMPSCI 172 or COMPSCI 174	INTRODUCTION TO JAVA INTRODUCTION TO C++	3
COMPSCI 220 or COMPSCI 222	INTERMEDIATE JAVA INTERMEDIATE C++	3
COMPSCI 223	DATA STRUCTURES	3
Core Courses:		
COMPSCI 271	COMPUTER ORGANIZATION AND ASSEMBLY PROGRAMMING	3
COMPSCI 366	DATABASE MANAGEMENT SYSTEMS	3
COMPSCI 412	COMPUTER ORGANIZATION AND SYSTEM PROGRAMMING	3
COMPSCI 433	THEORY OF ALGORITHMS	3
COMPSCI 476	SOFTWARE ENGINEERING	3
Electives: [2]		**12**
Any COMPSCI courses numbered 300 or above (no limit)		
Up to 6 total units in this category may come from the following courses:		
MATH 355	MATRICES AND LINEAR ALGEBRA	
MATH 450	GRAPH THEORY	
MATH 471	NUMERICAL ANALYSIS	
STAT 342	APPLIED STATISTICS	
Total Units		**36**

Figure 2 shows a sample course description that lists course prerequisites. Going through a text file to look for classes that need to be completed is time consuming and the advisor has to check course perquisites to make sure that the student is eligible to take each of the planned courses.

Figure 2. *Sample Course Description that Lists Prerequisites*

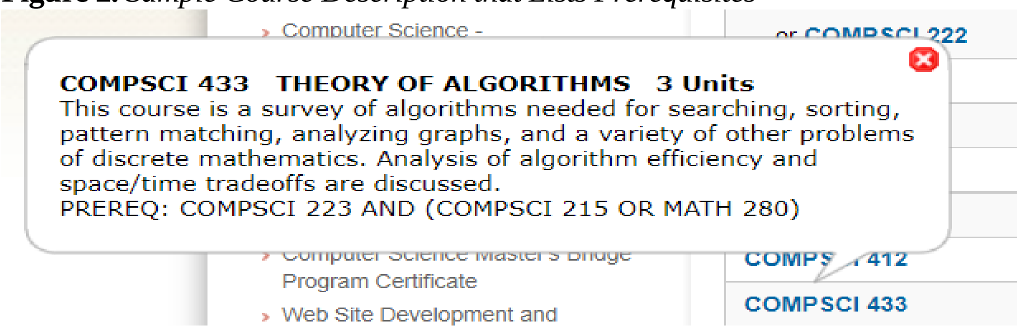

We use a predefined pattern to store a logical condition that defines dependencies on preceding nodes. For example, COMPSCI 223 and either COMPSCI 215 or MATH 280 must be completed before taking COMPSCI 433. We consider such a condition as completing two tasks *A* and *B* where *B* is also another task of completing one of the two tasks, task *C* or task *D*. We created an online graph visualization tool to evaluate course dependency structure, based on the requirements for each major. Since the courses that are completed by a student are stored in the database, this information can be used to display the current progress for each student using a directed graph. Students meet with their academic advisor to create a semester plan prior to enrolling for courses each semester. Using this visualization tool, the student and the advisor can easily explore the possible courses to take, based on the prerequisites and completed courses.

Figure 3 shows an implementation of our DVT which is based on the work by Samaranayake and Gunawardena (2020) to allow students to visualize degree paths. The objective is to display course dependencies to help computer science majors create a degree plan. In this implementation, we use a single node to represent a list of courses from which a subset of those courses needs to be completed. If two or more arrows are pointing to the same child node, then all the parent nodes are prerequisites to the child node. Courses shown in blue are the elective courses.

Figure 3. *Course Prerequisite Structure*

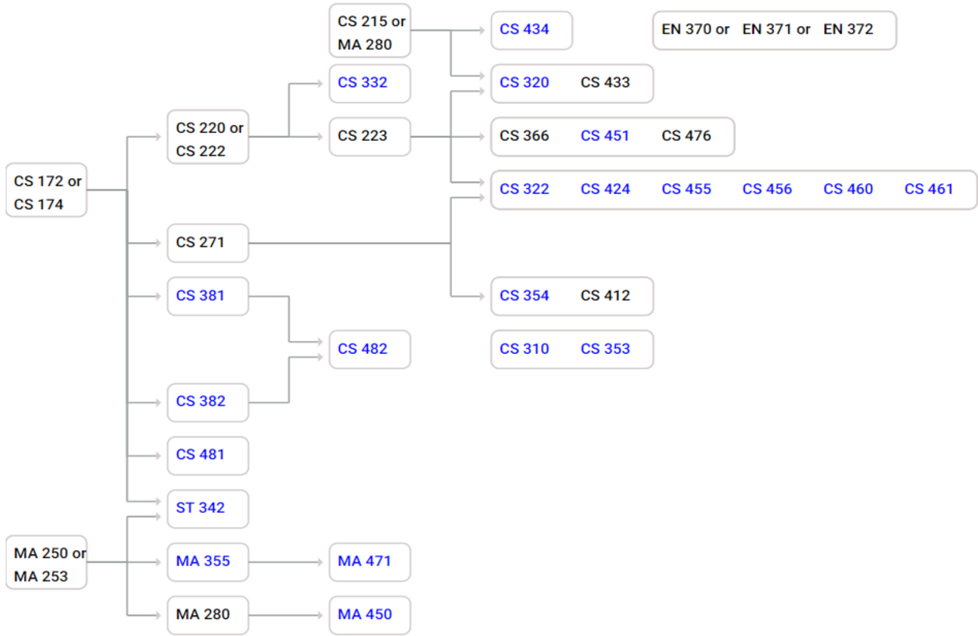

Computer science majors at UWW should complete 12 courses in order to satisfy the major requirements. There are more than 15,000 ways of completing those 12 courses: three courses in software development fundamentals, five core courses, and four of the elective courses. Many of the core courses and elective courses have common course dependencies. Hence, planning courses to create a degree path without using any visualization tools is a tedious and time-consuming process.

In general, graph representation is not unique. Hence, dependencies can be represented by many different directed graphs, based on user preferences or the type of dependencies. Suppose a particular task is defined as completing a subset of many predefined subtasks. We may have to use a separate path for each of those subtasks that have different predecessors. We will have to use a separate path for each subtask if we prefer to display all possible paths. Hence, the graph representation may depend on the user requirements, task dependencies, and/or type of the information represented by the system. For example, condition for fulfilling course dependencies of COMPSCI 433 (CS 433), as shown in Figure 2, can be defined using three subtasks: completing CS 223, CS 215, and MA 280. In Figure 3, those dependencies are displayed using different paths for each subtask that has a different predecessor. The prerequisite condition for CS 482 is to complete both CS 381 and CS 382, and those dependencies are displayed in Figure 3 using a separate path for each subtask even though they are two subtasks with the same predecessor. In this example, the choice of the path depends on whether subtasks are predecessors to multiple tasks or not.

Students are required to select 4 of the 22 elective courses for the computer science major. Students may select those 4 elective courses based on their course preferences, career goals, schedule preferences, or to optimize the time to graduate.

The data model is capable of dynamically updating the directed graph by adding new nodes to the graph or removing existing nodes from the directed graph. Hence, our tool provides a mechanism to filter elective courses based on their career goals or other preferences. Figure 4 shows a list of suggested elective courses from which students may complete four courses if they plan on pursuing graduate studies.

Figure 4. *Dynamic Filtering of Suggested Elective Courses*

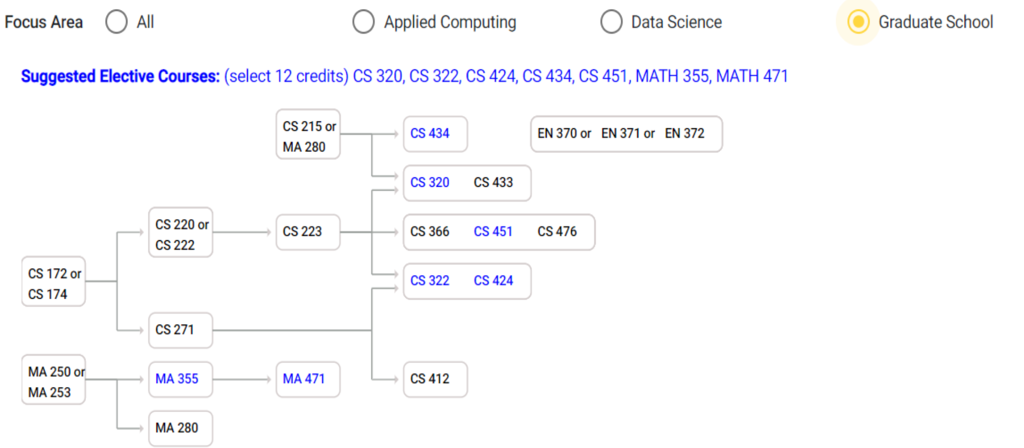

The data model that is used to generate these DVTs allows us to store the directed graph so that we can dynamically modify the node structure. Hence, the course prerequisite structure can be updated at the end of each semester to help students select courses based on the updated dependencies. Figure 5 shows a dynamically updated course prerequisite structure which is being used for academic advising. The course structure is updated dynamically to narrow down the course choices, based on the completed and planned courses. Course grades are displayed where * represents grades for the courses that are in progress. The courses shown in orange are the courses whose prerequisites are satisfied, and the courses shown in purple are the courses planned for the next semester. Green arrows point to courses that are available to take in the next semester. Two arrows pointing to the same block means both predecessors must be completed before starting the successor.

Figure 5. *Dynamically Updated Course Prerequisite Structure*

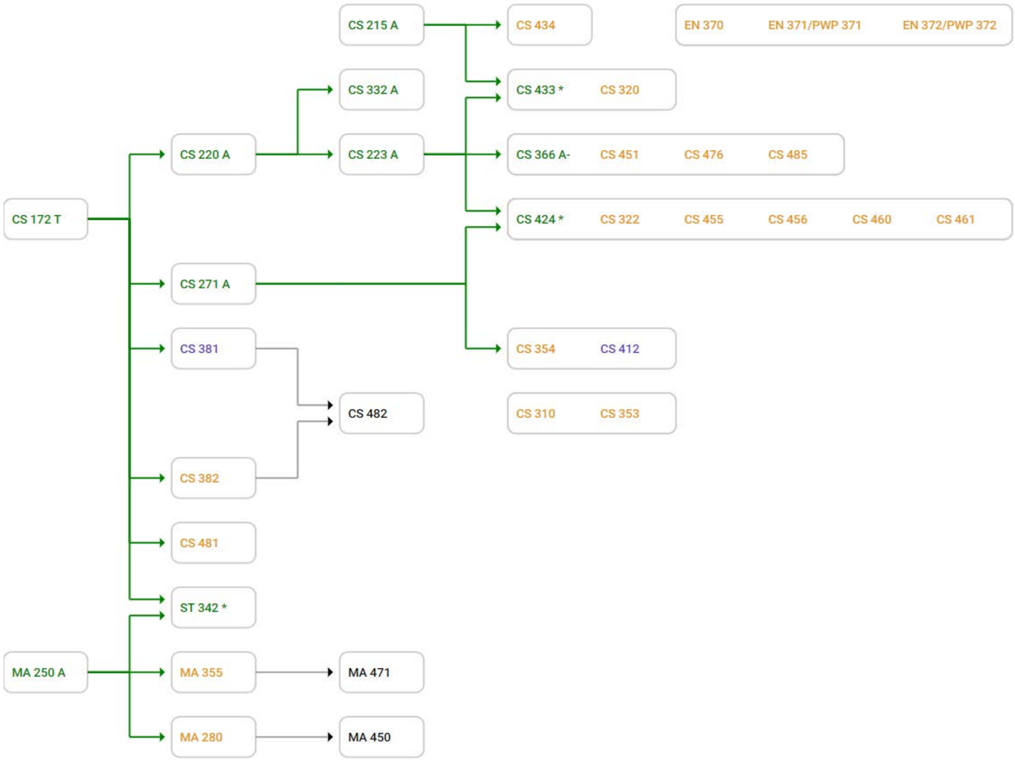

Visualization tools are extremely useful for identifying any bottleneck conditions that may prolong the completion of the process. For example, CS 223 and CS 271 are prerequisite courses for many of the 300-level or higher computer science courses. Hence, those two courses and their prerequisites must be completed as soon as possible to minimize the time to complete the degree.

The data model allows us to link each node to another directed graph. This feature is very useful for complex systems where each task is a subsystem that can be represented by our model. For example, Figure 3 includes a list of courses that can be used for planning the computer science major but there may be other hidden prerequisite courses that may not count for the computer science major. Figure 6 shows the implementation of course prerequisite structure for CS 172 and CS 174 as a directed graph linked to those two courses.

Figure 7 shows a directed graph of proficiency courses for different subject areas. This online application is being used to educate new students about the proficiency requirements for different subject areas. It is a very efficient method of sharing information that is usually scattered among many static documents.

Figure 6. *Course Prerequisite Structure for CS 172 and CS 174*

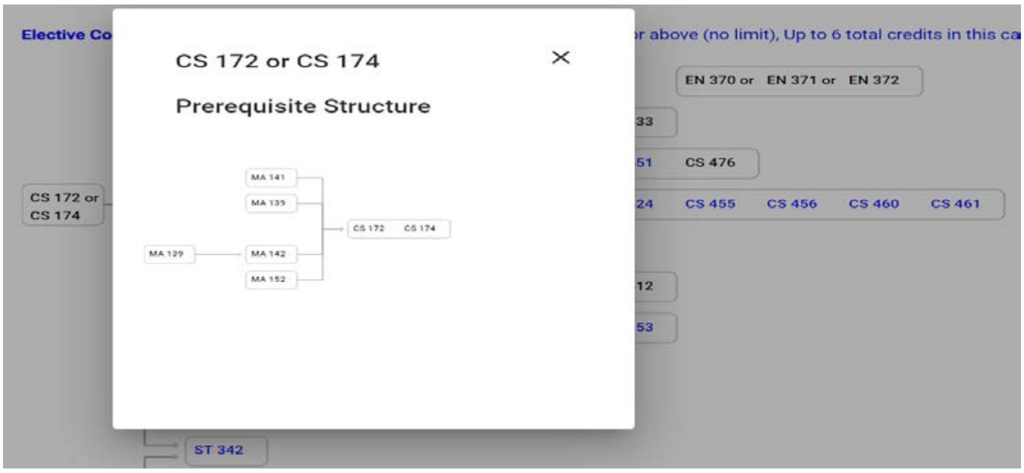

Figure 7. *Proficiency Course Structure*

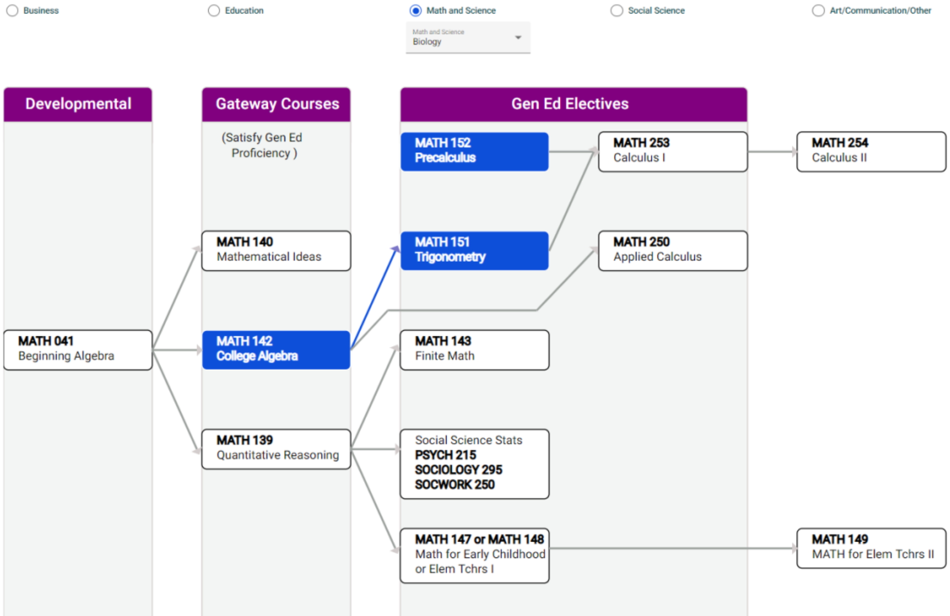

There are many such online applications where the DVTs are very useful for helping users make decisions. DVTs are also useful for managing long-term projects with multiple different ways to get to the end goal where the use of the flow chart can help project managers view current progress and preferential paths for project completion.

The data model we incorporate to generate these DVTs is very powerful and flexible. It allows us to dynamically modify the nodes and edges, format arrows connecting the nodes, and apply themes to format the appearance. Additionally, the orientation of the graph can be modified by applying rotations.

Conclusions

We present an online DVT which is useful for analyzing interactive systems with preferential dependencies, such as interest-aligned degree planning, project management, or career planning. Our implementation of the online DVT system to visualize the course prerequisite structure proved to be very effective and significantly faster than the traditional method of looking up indirect course dependencies and doing reverse prerequisite lookups. DVT system was able to help students quickly and easily find answers to questions like "If I have taken these courses, then what courses can I take next?" or "Why cannot I take this course yet?". Furthermore, the DVT helped students to identify the bottleneck scenarios in course planning. The DVT system that displays the proficiency course structure has been well received by academic advisors across several universities.

Data visualization tools are shown to be extremely useful for analyzing different scenarios to help make decisions about such systems. Also, online DVTs can help content management systems organize and display related information using a compact and efficient format. Furthermore, each node can represent a directed graph so the visualization tool can be used to analyze complex systems.

References

Al-Qaheri H, Hasan MK, Al-Husain R (2011) A decision support system for a three-stage university course scheduler with an application to College of Business Administration, Kuwait University. *International Journal of Data Analysis and Information Systems* 3(2): 95–110.

Alves CMO, Cota MP (2018) Visualization on decision support systems models: literature overview. *Advances in Intelligent Systems and Computing* 745: 730–740.

Anardani S, Sofyana LS, Maghfur A (2019) Analysis of business intelligence system design for student performance monitoring. *Journal of Physics Conference Series* 1381(1): 012015.

Basole RC, Huhtamäki J, Still K, Russell MG (2016) Visual decision support for business ecosystem analysis. *Expert Systems with Applications* 65(Dec): 271–282.

Burnay C, Dargam F, Zarate P (2019) Special issue: data visualization for decision-making: an important issue. *Operational Research* 19(Nov): 853–855.

Clark W (1922) *The Gantt chart: a working tool of management*. Ronald Press Company.

Faulkner A, (2018) Lucidchart for easy workflow mapping. *Serials Review* 44(2): 157–162.

Feng L (2016) Intelligent logistics and distribution system based on Internet of Things. In *2016 IEEE Advanced Information Management, Communicates, Electronic and Automation Control Conference (IMCEC)*, 228–231.

Hennocq Q, Khonsari RH, Benoît V, Rio M, Garcelon N (2021) Computational diagnostic methods on 2D photographs: a review of the literature. *Journal of Stomatology, Oral and Maxillofacial Surgery* 122(4): 71–75.

Horvath DM, Molontay R, Szabo M (2018) Visualizing student flows to track retention and graduation rates. In *2018 22nd International Conference Information Visualisation (IV)*, 338–343.

Huber TC, Krishnaraj A, Monaghan D, Gaskin CM (2018) Developing an interactive data visualization tool to assess the impact of decision support on clinical operations. *Journal of Digital Imaging* 31(5): 640–645.

Kerzner H (2003) *Project management: a systems approach to planning, scheduling, and controlling*. Hoboken, NJ: Wiley.

Krishnaiyer K, Chen FF (2017) Web-based visual decision support system for letter shop. *Robotics and Computer-Integrated Manufacturing* 43(Feb): 148–154.

Kuru K, Niranjan M, Tunca Y, Osvank E, Azim T (2014) Biomedical visual data analysis to build an intelligent diagnostic decision support system in medical genetics. *Artificial Intelligence in Medicine* 62(2): 105–118.

Lupton RC, Allwood JM (2017) Hybrid Sankey diagrams: visual analysis of multidimensional data for understanding resource use. *Resources, Conservation and Recycling* 124(Sep): 141–151.

Meyer RM, Gunawardena ADA, Samaranayake S, Deshpande V, Premadasa K (2021) Chapter 14: information technology for student decision support in College planning. In *Computing Technologies and Applications: Paving Path Towards Society 5.0*. Taylor & Francis Group.

Miranda J, Ray PA, Robles JM (2012) udpSkeduler: a web architecture based decision support system for course and classroom scheduling. *Decision Support Systems* 52(2): 505–513.

Morgan MB, Branstetter BF, Mates J, Chang P (2006) Flying blind: using a digital dashboard to navigate a complex PACS environment. *Journal of Digital Imaging* 19(1): 69–75.

Moscoso-Zea O, Castro J, Paredes-Gualtor J, Lujan-Mora S, (2019) A Hybrid infrastructure of enterprise architecture and business intelligence analytics for knowledge management in education. *IEEE Access* 7(Mar): 38778–38788.

Nevo D, Nevo S, Kumar N, Braasch J, Mathews K (2015) Enhancing the visualization of big data to support collaborative decision-making. In *2015 48th Hawaii International Conference on System Sciences*, 121–130.

Oladokun V, Oyewole DI (2015) A fuzzy inference based decision support system for solving the university-course admission choice problem. *International Journal of Computer Applications* 112(3): 10.5120/19643-1229.

Oran A, Martin A, Klymkowsky M, Stubbs R (2019) *Identifying students' progress and mobility patterns in higher education through open-source visualization*. Working Paper. University Administration Faculty and Staff Contributions, 1.

Parker DJ (2016) *Mastering data visualization with Microsoft Visio professional 2*016. Packt Publishing Ltd.

Power DJ (2008) Decision support systems: a historical overview. In *Handbook on Decision Support Systems 1. International Handbooks Information System*, 121–140. Berlin, Heidelberg: Springer.

Power DJ (2013) Mobile decision support and business intelligence: an overview. *Journal of Decision Systems* 22(1): 4–9.

Rouhani S, Ashrafi A, Ravasan AZ, Afshari S (2018) Business intelligence systems adoption model: an empirical investigation. *Journal of Organizational and End User Computing (JOEUC)* 30(2): 43–70.

Roushan T, Chaki D, Hasdak O, Chowdhury M, Annajiat A, Rahman M, et al. (2014) University course advising: Overcoming the challenges using decision support system. In *16th International Conference on Computer and Information Technology (ICCIT),* 13–18.

Samaranayake S, Gunawardena ADA (2020) Dependency evaluation and visualization tool for systems represented by a directed acyclic graph. *International Journal of Advanced Computer Science and Applications* 11(7): 1–7.

Siddiqui AW, Raza SA, Tariq ZM (2018) A web-based group decision support system for academic term preparation. *Decision Support Systems* 114(Oct): 1–17.

Sugumaran, V, Sugumaran R (2007) Web-based spatial decision support systems (WebSDSS): evolution, architecture, examples and challenges. *Communications of the Association for Information Systems* 19(1).

Trase K, Fink E (2014) A model-driven visualization tool for use with model-based systems engineering projects. In *2014 IEEE Aerospace Conference*, 1–10.

Trieu V (2017) Getting value from business intelligence systems: a review and research agenda. *Decision Support Systems* 93(Jan): 111–124.

West VL, Borland D, Hammond WE (2015) Innovative information visualization of electronic health record data: a systematic review. *Journal of the American Medical Informatics Association* 22(2): 330–339.

Wright A, Bates DW, Middleton B, Hongsermeier T, Kashyap V, Thomas SM, et al. (2009) Creating and sharing clinical decision support content with Web 2.0: Issues and examples. *J Biomed Inform* 42(2): 334–346.

Vo TNC, Nguyen HP (2012) A knowledge-driven educational decision support system. In *2012 IEEE RIVF International Conference on Computing & Communication Technologies, Research, Innovation, and Vision for the Future*, 1–6.

Athens Journal of Technology and Engineering - Volume 9, Issue 4, December 2022 – Pages 281-304

Numerical Estimation of a Mode III Fracture Mechanics Parameter for a Three-Dimensional V-Notch on a Steel Bold

By Miltiades C. Elliotis[*]

In this work a couple of three-dimensional problems in the domain of linear elastic Fracture Mechanics are examined. These are problems of solid bodies (they could be steel bolds or rivets) with a surface crack singularity (V-notch). They are reduced to Laplace equation problems by considering a Lamé potential. The boundary singularity is numerically treated as per the singular function boundary integral method (SFBIM), which in the literature is known as one of the so-called Trefftz methods. Thus, the general solution of the governing equation, in the vicinity of the surface crack, is expressed as an asymptotic expansion, the coefficients of which are approximated by polynomials. The remaining numerical steps are followed according to this method with which very fast convergence and very high accuracy are observed. In fact, the CPU time and the numerical error recorded with this numerical technique are significantly smaller than those achieved with the finite element method (FEM) which was also used to solve the same problems. The calculated value of Mode III Fracture Mechanics parameter (FMP) indicates that there is no danger of crack propagation. Thus, the extension of the method to this category of problems is considered as a novel application of this algorithm in Fracture Mechanics.

Keywords: *Mode III Fracture Mechanics parameter, crack singularity, governing equation, singular function boundary integral method, local solution, Lamé potential*

Introduction

Force formulation in linear elasticity problems is not an easy task. Our attempt to overcome difficulties encountered in this category of engineering problems is a great challenge when we have to tackle three-dimensional problems. Such problems are treated by professionals and researchers in the fields of engineering, such as the construction industry, mechanical engineering, car industry and aerospace engineering. Their number is continuously growing due to the needs for new complicated structures, such as construction trusses, geodesic domes and tensegrity structures, mechanisms (made of metal alloys) used in robotics and biomedical engineering, vehicles and aircrafts with sensitive and complicated mechanical connections and many others. Thus, most engineering problems in the domain of Solid Mechanics are three-dimensional problems which lead the designers and researchers to the implementation of approaches which exhaust the

[*]Scientific Collaborator, Department of Mathematics and Statistics, University of Cyprus, Cyprus.

limits of computational resources. Also, in trying to solve particular problems in the fields of theoretical or applied Mechanics, exhibiting specific boundary singularities, engineers have to overcome several obstacles. Such problems are the elliptic equation problems of fracture Mechanics with boundary discontinuities or crack singularities.

In some model problems of linear elasticity, in the three-dimensional space, the governing equation is the so-called Beltrami-Michel equation of a three-variable function, which is known as "stress invariant" and is a function of the body forces each one acting along *x*, *y* or *z* axis:

$$\nabla^2\sigma_{ij} + \frac{1}{1+\nu}\frac{\partial^2\left(\sum_{k=1}^{3}\sigma_{kk}\right)}{\partial x_i \partial x_j} = -\frac{\nu}{1-\nu}\delta_{ij}\left(\sum_{k=1}^{3}\frac{\partial f_k}{\partial x_k}\right) - \left(\frac{\partial f_i}{\partial x_j} + \frac{\partial f_j}{\partial x_i}\right) = $$
$$= -\frac{\nu}{1+\nu}\delta_{ij}\nabla^2 Q_1 - \left(\frac{\partial f_i}{\partial x_j} + \frac{\partial f_j}{\partial x_i}\right) \quad i, j = 1,2,3 \tag{1}$$

where ν is the Poisson ratio, σ_{ij} are the stresses, Q_1 is the first stress invariant and f_1, f_2 and f_3 are body forces. In some problems body forces are constant and thus the above equation is deduced to the following form:

$$\nabla^2\sigma_{ij} + \frac{1}{1+\nu}\frac{\partial^2\left(\sum_{k=1}^{3}\sigma_{kk}\right)}{\partial x_i \partial x_j} = \nabla^2\sigma_{ij} + \frac{1}{1+\nu}\frac{\partial^2 Q_1}{\partial x_i \partial x_j} = 0 \tag{2}$$

Thus, according to the compatibility condition, the governing equation is $\Delta(Q_1) = 0$. But it is well known that complexities appear when there are boundary singularities which form a particular type of problems.

In engineering mechanics, this type of problems is of great importance because boundary singularities affect seriously the regularity of the solutions, leading to convergence irregularities and low accuracy which is dispersed in all the domain of the problem. During the last decade of the 20th century several techniques have been developed (e.g., Aliabadi and Rooke 1991, Li 1998) aiming to efficiently and effectively tackle this category of problems. In many applications it is important to know in advance the values of the coefficients of all the leading terms appearing in the local solution, which is expressed in series form (Costabel et al. 2003, Szabo and Yosibash 1996) because they are related to other important parameters found in Fracture Mechanics (Aliabadi and Rooke 1991), such as the Mode III FMP. Obviously, knowledge of the values of these parameters enables the designers and engineers to decide about the appropriate materials and dimensions to use according to the anticipated loading and thermal conditions of the structure. In addition, it is also important to have a good knowledge of the type of boundary singularities, in order to tackle them in the most appropriate way (Fung 1977). In two-dimensional elliptic boundary value problems sometimes appear two types of boundary singularities (Figure 1). The first type is a discontinuity in the boundary conditions (an abrupt change in the boundary conditions around a point) mainly caused by a crack. The second type is a re-entrant corner.

Figure 1. *Two Types of Planar Singularities*

Discontinuous BCs (cracks) **Re-entrant corners**

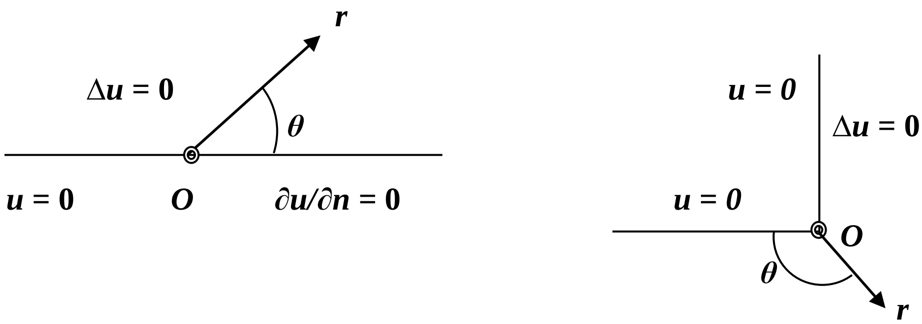

The local solution, in the neighborhood of the singularity of a two-dimensional problem, is expressed in the form of an asymptotic expansion in terms of the singular coefficients a_j which are the primary unknowns:

$$u = \sum_{j=1}^{\infty} a_j r^{\mu_j} U_j(\theta) \tag{3}$$

where $U_j(\theta)$ is the singular function and μ_j are the eigen-values of the problem.

A large number of numerical techniques, which appear in the literature, are based on post-processing of the numerical solution, such as the *p-hp* Finite Element Method or other finite element schemes (Seshaiyer and Suri 1998, Stephan and Whiteman 1988, Brannick et al. 2008, Brenner 1999, Brenner and Scott 1994) the accuracy and convergence rate of which are not adequate enough. However, the general idea of these methods is that the boundary singularity is considered in the design of the finite element grid by employing an appropriate refinement and the values of the coefficients of the local solution are extracted by implementing post-processing, something which is not required with boundary element methods. The latter were initially developed to tackle planar problems and they do not require complicated grids. Also, they are applied on the boundary of the domain (Karageorghis 1992, Katsikadelis 1991).

The so-called Trefftz methods (Bernal and Kindelan 2010, Li et al. 2007, Li et al. 2008) belong to this type of mesh-less numerical techniques and are based on local solutions (e.g., equation (3)) or basis functions which satisfy the governing equations and thus allow collocation to be conducted only on the boundary. These are the main characteristics of this category of methods which make them more appropriate than the post-processing methods. In Li et al. (2008) it is explained that the main advantages of the Trefftz methods over the FEM and finite difference methods, include their flexibility in representing the boundary singularities and irregular geometry of the problem domains, ease of data input and pre-processing, high accuracy of the numerical solution and efficient computation. In the same reference it is mentioned that especially for the collocation Trefftz method (CTM) it has been shown that it is a more accurate numerical technique compared with other numerical methods (including the post-processing methods) not only for the global solution but also for the leading coefficients of the local solution expansion, something which is important in problems of Fracture Mechanics.

The singular function boundary integral method (SFBIM) is a Trefftz method and is used in the present work. Its fundamental characteristic is that the solution is approximated by the leading terms of the local asymptotic series around the boundary singularity. It has been developed by G. Georgiou and co-workers and has been used in many studies to tackle planar harmonic and biharmonic equation problems and three-dimensional Laplace equation problems in the fields of theoretical and fracture Mechanics, fluid flow, etc. (Christodoulou et al. 2012a, b, Elliotis et al. 2010, Elliotis et al. 2002, Elliotis et al. 2005a, b, Elliotis et al. 2006, Elliotis et al. 2007, Elliotis et al. 2014, Elliotis 2016, Elliotis 2019, Georgiou et al. 1996, Xenophontos et al. 2006). It exhibits exponential convergence, a feature which was observed in all previous applications of the method. Its application in three-dimensional problems (Christodoulou et al. 2012b, Elliotis et al. 2010, Elliotis 2016), has given much encouragement to extend the method to other three-dimensional Laplacian problems of perfectly elastic solid bodies with a crack singularity. Also, in the last five or six years, researchers have worked on problems of Fracture Mechanics with crack singularities and have obtained interesting results (Yosibash and Mittelman 2016, Schapira and Yosibash 2020, Omer and Yosibash 2019, Yosibash and Schapira 2021, Chaumont-Frelet and Nicaise 2018, Dauge and Nicaise 2017, Woo and Kim 2018). Following the same research interests, in the present work, we also examine the behavior of solid bodies when they develop a specific failure mode of Fracture Mechanics.

It is well known that in Fracture Mechanics there are three failure Modes (Aliabadi and Rooke 1991): Mode I (opening Mode), Mode II (in-plane shear Mode) and Mode III (out-of-plane shear Mode) which is the failure type examined in the current research (Figure 2). There is a very rich literature around these failure Modes in which the stress intensity factors play an important role in engineering analysis and calculations for the design of structures. In the present study we are interested in Failure Mode III.

Figure 2. *The Three Types of Failure Modes in Fracture Mechanics*

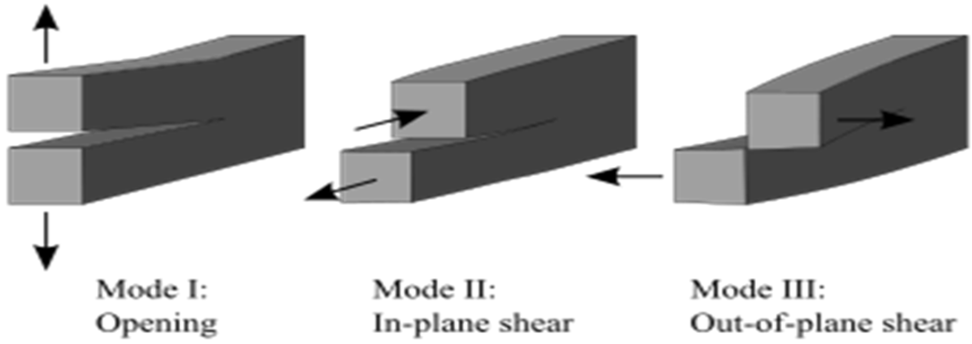

The rest of the article is organized as follows: in the next section a general 3-D Laplace equation problem of a solid body made of steel, with a crack singularity and a specific 3-D model problem of a steel rivet with a surface V-notch (singularity) are presented. Then, the general form of the local solution is given and the three-dimensional version of the SFBIM formulation, for the general and specific model problems, is presented. Numerical results are presented and discussed afterwards. Finally, in the last section, the conclusions are summarized.

The goal of this article is to present the extension of the SFBIM in Fracture Mechanics to efficiently solve the two problems of solid bodies, with a surface crack singularity (V-notch), exhibiting a failure Mode III. Also, the objective of the present study is to prove that, for the specific two problems, this method is much faster (i.e., it requires much smaller CPU time) and is much more accurate than the finite element method (FEM) which is still widely used by engineers and researchers by employing commercial packages. The novelty in the present study is that the SFBIM is extended in 3-D problems of Fracture Mechanics, exhibiting great advantages over the FEM. This encourages a further extension in this field of Mechanics.

General and Specific Model Problems

General Model Problem

In Figure 3 a general 3-D model problem of a solid body is presented. It has a straight-edge crack-singularity which is created by the intersection of two flat boundary parts S_A and S_B. In fact, this singularity is a straight line parallel to the Z-axis and at a distance d_c from this axis. The value of d_c can be varied. Both boundaries S_A and S_B form an angle φ_A with the XZ plane (i.e., S_B is symmetric to S_A with respect to the XZ plane). The external angle ω_d (as shown in Figure 3), between these two boundary parts, takes values in a certain range of values $[0.0002\pi,\ 1.9998\pi]$. Both ω_d and φ_A are measured in a local polar coordinate system $(r,\ \theta)$, with center O_d on boundary part S_D or K_d on S_E. Any other center of a local polar coordinate system, on a cross-section parallel to S_D and S_E, lies on the straight-edge crack-singularity. Flat boundaries S_D and S_E, on each one of the two ends of the solid body, are vertical to both the *Z*-axis and the edge singularity and located at a distance *L* between them. The domain of the problem is also bounded by a boundary part S_C. It forms the cylindrical shape of the solid of the problem which has a cross-section with a circumference represented by the equation of an ellipse (Figure 3). Certainly, it retains a constant shape along *Z*-axis.

Figure 3. *Schematic Illustration of the Domain of the General Model Problem*

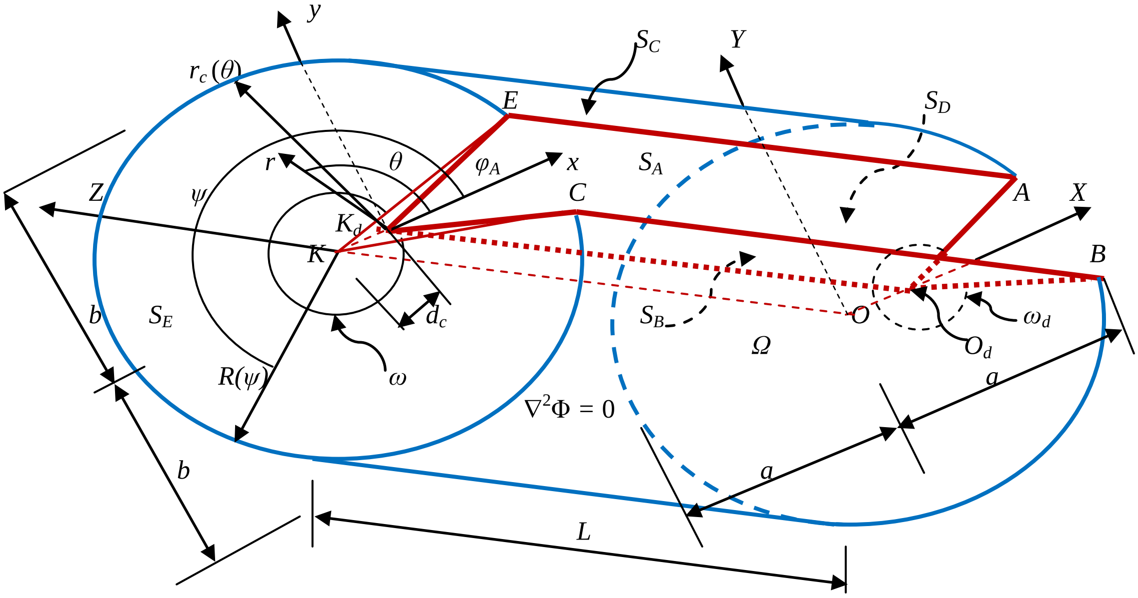

In Figure 3 the fundamental parameters ψ and $R[\psi(\theta)]$, employed in this problem, for the cylindrical co-ordinates, are defined as follows:

$$\psi = tan^{-1}\left(\frac{r_c(\theta)\,sin(\theta)}{d_c + r_c(\theta)\,cos(\theta)}\right), \qquad R[\psi(\theta)] = \frac{ab}{\sqrt{a^2\,sin^2[\psi(\theta)] + b^2\,cos^2[\psi(\theta)]}} \tag{4}$$

where *a* and *b* are the dimensions of the two axis of the elliptic cross-section.

The material of this solid body is isotropic homogeneous and obeys to Hooke's law. Also, there are no body forces. Thus, there is a scalar function $\Phi_g(r,\theta,z)$, known as Lamé strain potential function, which reduces the linear elasticity equations to the Laplace operator and is always independent of the values of Young's modulus *E* and the Poisson ratio *v* of the material (Fung 1977). Also, as per Fung (1977), the potential function generates the field of stresses (stress tensor). According to the same reference, which is one of the known classical books about theoretical Mechanics, stresses σ_{rr}, $\sigma_{\theta\theta}$, σ_{zz}, $\sigma_{r\theta}$, $\sigma_{\theta z}$ and σ_{zr} and displacements ξ_r, ξ_θ and ξ_z are expressed in cylindrical coordinates in terms of function $\Phi_g(r,\theta,z)$ as follows (with *G* being the shear modulus and defined as $G = \frac{E}{2(1+\nu)}$):

$$\begin{aligned} &\sigma_{rr} = \partial_r^2\Phi_g, && \sigma_{\theta\theta} = r^{-1}\partial_r\Phi_g + r^{-2}\partial_\theta^2\Phi_g, && \sigma_{zz} = \partial_z^2\Phi_g \\ &\sigma_{r\theta} = \partial_r\left(r^{-1}\partial_\theta\Phi_g\right), && \sigma_{\theta z} = r^{-1}\partial_\theta\left(\partial_z\Phi_g\right), && \sigma_{zr} = \partial_z\left(\partial_r\Phi_g\right) \\ &\xi_r = (1/2G)\partial_r\Phi_g, && \xi_\theta = (1/2G)r^{-1}\partial_\theta\Phi_g, && \xi_z = (1/2G)\partial_z\Phi_g \end{aligned} \quad (5)$$

The mathematical conditions can be derived from the physical conditions of the problem. Thus, the mathematical problem is expressed as follows: Find $\Phi_g(r,\theta,z)$ such that

$$\nabla^2\Phi_g = \Delta\Phi_g = 0 \quad in \quad \Omega \quad (6)$$

with the following physical and mathematical conditions:

$$\left.\begin{aligned} &\sigma_{\theta\theta}(r,z) = 0 && or && \Phi_g = 0 && on \quad S_A \\ &\xi_\theta(r,z) = 0 \ (no\ distortion) && or && \partial_\theta\Phi_g = 0 && on \quad S_B \\ &\sigma_{rr} = p(\theta,z) = \partial_r^2(\Phi_g(r,\theta,z))\Big|_{r\to R(\theta)} && or && \Phi_g = f_g(\theta,z) && on \quad S_C \\ &\delta_D(r,\theta) = \xi_z\big|_{S_D} = -\xi(r,\theta), && or && \partial_z\Phi_g = -2G\xi(r,\theta) && on \quad S_D \\ &\delta_E(r,\theta) = \xi_z\big|_{S_E} = \xi(r,\theta), && or && \partial_z\Phi_g = 2G\xi(r,\theta) && on \quad S_E \end{aligned}\right\} \quad (7)$$

Lamé potential $\Phi_g(r,\theta,z)$ is not known for this general model problem with boundary singularity. The expressions of functions $f_g(\theta,z)$ and $\xi(r,\theta)$ are as follows:

$$f_g(\theta,z) = \Phi_g(r,\theta,z)\Big|_{r\to r_c(\theta)} = \sum_{k=1}^{2}\left[\sum_{j=1}^{2} a_{k,j} z^{j-1}\right] r_c(\theta)^{\frac{(2k-1)\pi}{2(\omega_d-\varphi_A)}} \sin\left(\frac{(2k-1)\pi}{2(\omega_d-\varphi_A)}\varphi(\theta)\right), \quad (8)$$

$$\varphi_A \le \theta \le \omega_d, \quad \omega_d = 2\pi - 2\varphi_A$$

$$\xi(r,\theta) = \frac{1}{2G}\sum_{k=1}^{2}\left[\partial_z\left(\sum_{j=1}^{2} a_{k,j} z^{j-1}\right)\right] r^{\frac{(2k-1)\pi}{2(\omega_d-\varphi_A)}} \sin\left(\frac{(2k-1)\pi}{2(\omega_d-\varphi_A)}(\theta-\varphi_A)\right) \quad (9)$$

Specific Model Problem of a Steel Rivet with a Surface V-notch

The general model problem discussed in the previous subsection is now specialized into a model problem of a solid body schematically illustrated in Figure 4. As a special case of the more general problem of the previous sub-section, the values of a and b (Figure 3) are now equal to each other and each point of the circumference of any circular cross section, on cylindrical boundary S_C, is at equal distance from the z-axis. The solid body of this particular model problem is a metal rivet with a circular cross section of radius R=1cm, which connects three steel members of a structure to create a joint. Its middle part has a length L=2 cm and is transmitting an eccentric load which comes from the middle element. Thus, its cylindrical surface is subjected to a distributed load $q(\theta,z)$ which is acting along the radial direction and is expressed in *MPa* (a common unit of pressure).

Figure 4. *Schematic Illustration of the 3-D Image and Layout of Joint (Specific Model Problem of a Steel Rivet with a V-notch)*

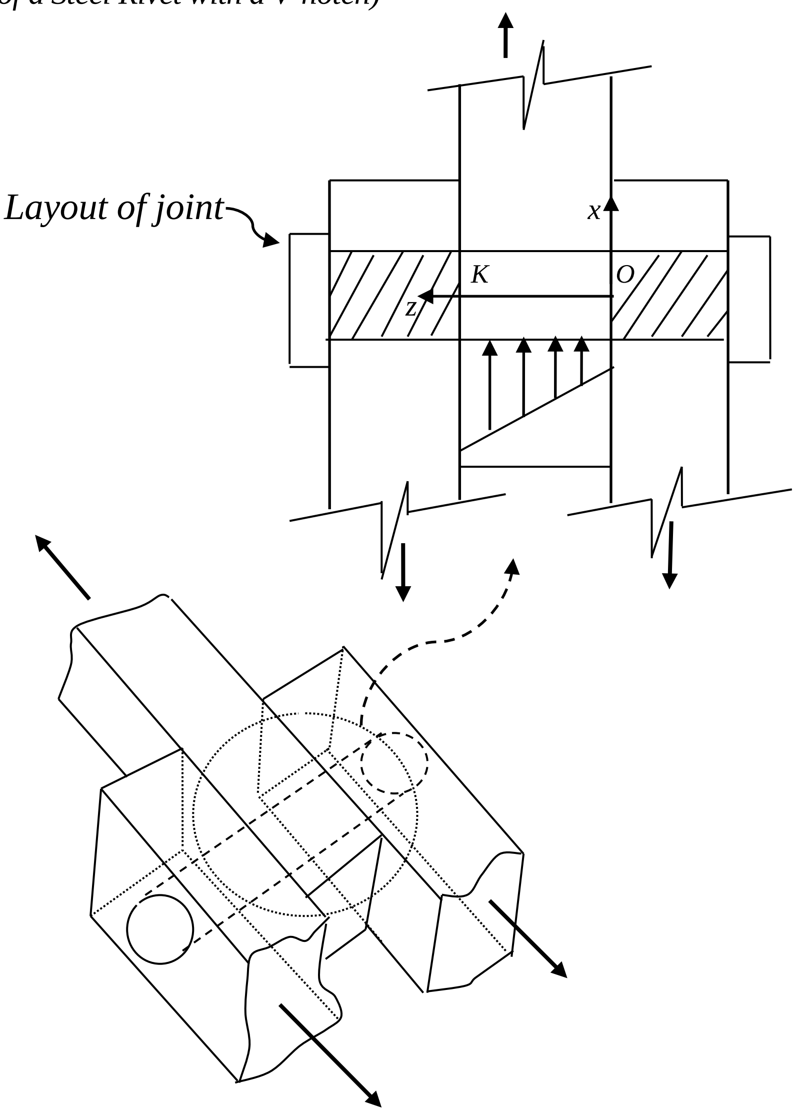

There is a crack on this solid body, represented by a V-notch which can propagate under certain stress and strain concentration states and in general has its vertex on a line parallel to the axis of the cylinder (*z*-axis) at a distance d_c. In the current work it is investigated whether the applied loading activates crack propagation. As we will see, after several numerical experiments, distance d_c is finally taken equal to zero. This choice is made in order to study the worst case of crack formation of Mode III in the steel rivet of this specific problem. Engineering experience indicates that under certain loading conditions further crack propagation, in this particular case, most probably leads the material to a failure (Aliabadi and Rooke 1991), something which will be also examined in the present study together with other material properties. Together with the distributed load there is a displacement $\xi(r,\theta)$ which takes place along the *z*-axis on each one of the cross sections at positions K and O (Figure 4). The self-weight of the body is negligible compared with other loads and is ignored. Therefore, there are no body forces.

According to the description of the physical problem given above, the principal physical boundary conditions are as follows:

$$\left.\begin{array}{lll} \sigma_{\theta\theta} = 0, & on & S_A \\ \xi_\theta = 0, & on & S_B \\ \sigma_{rr} = q(\theta, z), & on & S_C \\ \xi_z\big|_{S_D} = -\xi(r,\theta), & on & S_D \\ \xi_z\big|_{S_E} = \xi(r,\theta), & on & S_E \end{array}\right\} \quad (10)$$

where the stresses σ_{rr}, $\sigma_{\theta\theta}$ and σ_{zz} and the displacements ξ_θ and ξ_z can be easily deduced from $\Phi_s(r,\theta,z)$ which is known for this problem (Fung 1977) and is expressed in cylindrical coordinates. Considering boundary conditions (10) the problem is specialized as follows: Find Φ_s such that

$$\nabla^2\Phi_s = \Delta\Phi_s = \partial_r^2\Phi_s + r^{-1}\partial_r\Phi_s + r^{-2}\partial_\theta^2\Phi_s + \partial_z^2\Phi_s = 0 \quad in \quad \Omega \quad (11)$$

$$\left.\begin{array}{lll} \Phi_s = 0, & on & S_A \\ \partial_\theta\Phi_s = 0, & on & S_B \\ \Phi_s = f_s(\theta,z) & on & S_C \\ \partial_z\Phi_s = -\zeta(r,\theta), & on & S_D \\ \partial_z\Phi_s = \zeta(r,\theta), & on & S_E \end{array}\right\} \quad (12)$$

where $\zeta(r,\theta) = 2G\xi(r,\theta)$. Also, for $d_c \neq 0$ functions $f_s(\theta,z)$, $\zeta(r,\theta)$, $\Phi_s(r,\theta,z)$ and $q(\theta,z)$ have the following mathematical expressions:

$$f_s(r,\theta,z)\Big|_{r\to r_c(\theta)} = \sum_{k=1}^{2}\left[\sum_{j=1}^{2} a_{k,j} z^{j-1}\right] r^{\frac{(2k-1)\pi}{2(\omega_d-\varphi_A)}} \sin\left(\frac{(2k-1)\pi}{2(\omega_d-\varphi_A)}(\theta-\varphi_A)\right)\Bigg|_{r\to r_c(\theta)}$$

$$where \quad r_c(\theta) = \left[\sqrt{R^2 - d_c^2\sin^2(\theta)} - d_c\cos(\theta)\right]_{R\to 1\,cm} \quad (13)$$

$$\zeta(r,\theta) = -\partial_z\Phi_s\Big|_{S_D} = \partial_z\Phi_s\Big|_{S_E} = 2\left[r^{\frac{\pi}{2(\omega_d-\varphi_A)}} \sin\left(\frac{\pi(\theta-\varphi_A)}{2(\omega_d-\varphi_A)}\right) + r^{\frac{3\pi}{2(\omega_d-\varphi_A)}} \sin\left(\frac{3\pi(\theta-\varphi_A)}{2(\omega_d-\varphi_A)}\right)\right] \quad (14)$$

$$\Phi_s(r,\theta,z) = (1+2z)\left[r^{\frac{\pi}{2(\omega_d-\varphi_A)}} \sin\left(\frac{\pi(\theta-\varphi_A)}{2(\omega_d-\varphi_A)}\right) + r^{\frac{3\pi}{2(\omega_d-\varphi_A)}} \sin\left(\frac{3\pi(\theta-\varphi_A)}{2(\omega_d-\varphi_A)}\right)\right], \quad (15)$$

$$q(\theta,z) = \partial_r^2(\Phi_s(r,\theta,z))\Big|_{r\to r_c(\theta)} \quad (16)$$

Note that all values of boundary conditions are dimensional: distributed loads are expressed in N/cm^2 and lengths in *cm* and can be easily converted into *MPa* and *m* respectively, which are common units in most engineering problems. As already mentioned, when parameter d_c is taken equal to zero it is $\omega_d=\omega$ and $r_c(\theta)=R=1$ *cm* and on any cross-section angle θ is measured from an axis parallel to the *x*-axis (Figure 5). Then for this specific case the above expressions take the following form (they can be also expressed in the Cartesian coordinate system but here they are expressed in the cylindrical coordinate system centered at the *z*-axis as shown in Figure 5):

$$q(\theta,z) = \partial_{rr}\left(f_s(r,\theta,z)\right)\Big|_{r\to 1\,cm} = \\ = (1+2z)\frac{\pi}{2\omega}\left[\left(\frac{\pi}{2\omega}-1\right)sin\left(\frac{\pi\theta}{2\omega}\right)+3\left(\frac{3\pi}{2\omega}-1\right)sin\left(\frac{3\pi\theta}{2\omega}\right)\right] \tag{17}$$

$$f_s(r,\theta,z)\Big|_{r\to 1\,cm} = (1+2z)\left[sin\left(\frac{\pi\theta}{2\omega}\right)+sin\left(\frac{3\pi\theta}{2\omega}\right)\right] \tag{18}$$

$$\zeta(r,\theta) = -\partial_z\Phi_s\Big|_{S_D} = \partial_z\Phi_s\Big|_{S_E} = 2\left[r^{\frac{\pi}{2\omega}}\,sin\left(\frac{\pi\theta}{2\omega}\right)+r^{\frac{3\pi}{2\omega}}\,sin\left(\frac{3\pi\theta}{2\omega}\right)\right] \tag{19}$$

$$\Phi_s(r,\theta,z) = (1+2z)\left[r^{\frac{\pi}{2\omega}}\,sin\left(\frac{\pi\theta}{2\omega}\right)+r^{\frac{3\pi}{2\omega}}\,sin\left(\frac{3\pi\theta}{2\omega}\right)\right] \tag{20}$$

Figure 5 depicts the mathematical form of this model problem and presents, mainly, its geometrical characteristics and the mathematical domain Ω_s of the above problem. Angle ω presented in the figure has maximum and minimum values equal to 1.998π *rads* and 0.002π *rads* respectively. Note that for very small values, such as $\omega=0.002\pi$ *rads*, the solid body becomes a blade. Also, in Figure 5, the schematic illustration of the distribution of the resulting surface tractions $q(r,\theta)$ on boundary S_C is presented. The distribution of surface traction at a cross section with z=1 cm, is also presented in the same figure. This external load distribution, which can be determined from the known solution, indicates that external loading on the solid body is not symmetric and causes bending to the central part of the rivet. Thus, apart from $q(r,\theta)$ additional stresses due to friction (shear stresses) and contact of the rivet with the middle steel member, appear on S_C.

Figure 5. *Specific Model Problem's Domain with Schematic Illustration (not to Scale)*

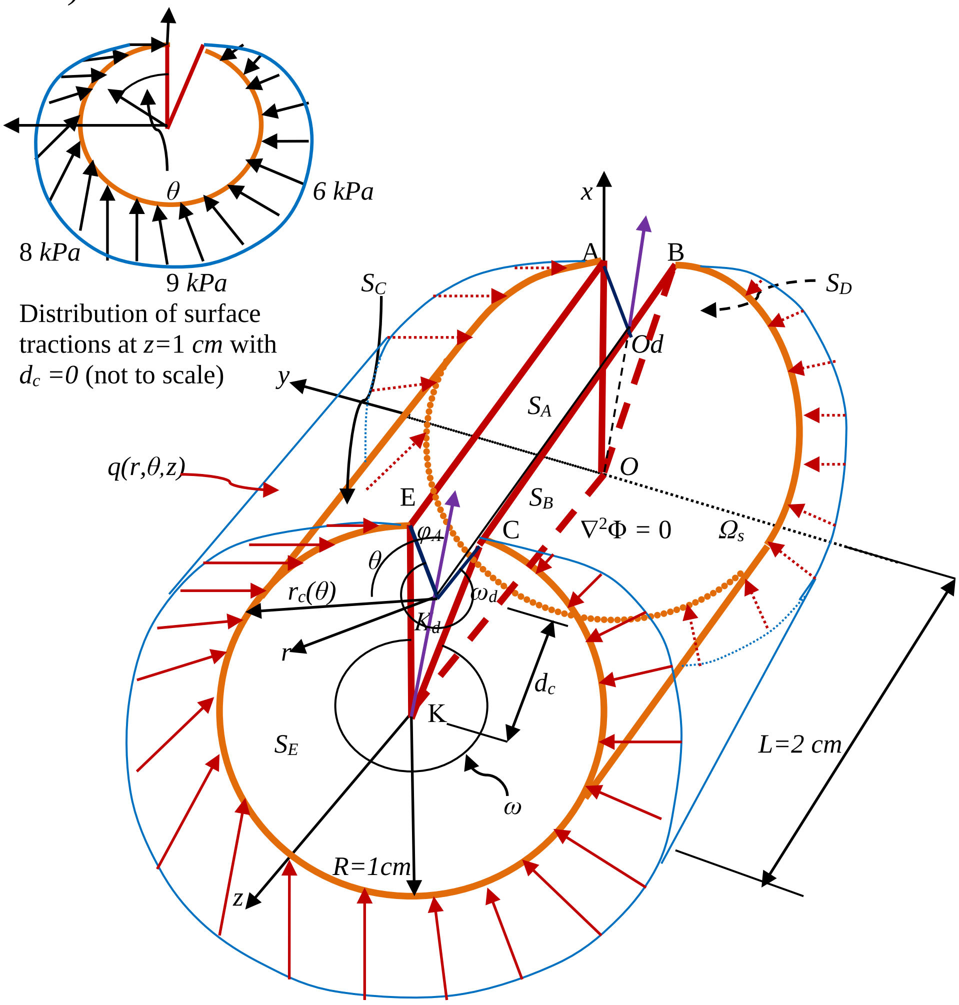

For this problem it is E=210GPa and v=0.30. Also, the material of the solid body is a high-yield steel of type S700MC, suitable for cold forming structural load-bearing components, with a titanium content of 0.22% and yield strength (elastic limit) σ_y=620MPa. Beyond this limit, elastic-plastic deformation appears.

A Boundary Integral Method in 3-D

Formulation of the Method

The solution Φ of the 3-D Laplace equation, is expressed in cylindrical coordinates and is defined in a domain with a boundary crack singularity along the *z*-axis or along a line parallel to this axis, as it is the case of the model problems which have been examined in the current study. It is written as follows (Costabel et al. 2003, Christodoulou et al. 2012b, Elliotis et al. 2010, Elliotis 2016):

$$\Phi(r,\theta,z)=\sum_{k=1}^{\infty}\left[\left(F^{(a_k)}(z)+\sum_{i=1}^{\infty}c_{k,i}\partial_z^{2i}\left(F^{(a_k)}(z)\right)r^{2i}\right)r^{a_k}\varphi_k(\theta,a_k)\right], \qquad (21)$$

In the present work, function Φ represents the Lamé strain potential function (Fung 1977) as has already been mentioned. The mixed boundary conditions on the boundary parts S_A and S_B, which share the boundary singularity, do not yield logarithmic terms in (21) because eigenvalues α_κ are not integers and there are no “crossing points”. Although both the general and specific model problems in Figures 3 and 5, have mixed boundary conditions on boundaries S_A and S_B which share the singularity, it is known that for the isotropic materials in 3-D linear elasticity, which is the case of our problems, the local solution expansion in the vicinity of the singularity does not contain any logarithmic terms (Costabel et al. 2003).

In elliptic coordinates, as it is the case of the general model problem, the singular solution may be found by following the theory developed in Li et al. 2008. According to the same reference the elliptic coordinates fail to present the concave corners with $\theta<2\pi$. Thus, we have to solicit the singular solution in cylindrical coordinates. Moreover, for the general model problem and as per Li et al. (2007) and Li et al. (2008), expression (21) is preferred for simplicity. Now, in (21) functions $F^{(a_k)}(z)$ are polynomials of degree N_p and with unknown coefficients $a_{k,j}$ and are expressed as follows:

$$F^{(a_k)}(z)=\sum_{j=1}^{N_p+1}\alpha_{k,j}z^{j-1} \qquad (22)$$

The eigenfunctions $\varphi_\kappa(\theta,\alpha_\kappa)$ and the eigenvalues α_κ in (21) are given by

$$\varphi_k(\theta,a_k)=sin\left(a_k(\theta-\varphi_A)\right), \quad a_k=\left((2k-1)\pi\right)/\left(2(\omega_d-\varphi_A)\right) \quad k=1,2,\cdots \qquad (23)$$

where ω_d is shown in Figures 3 and 5. Also, for the specific model problem the first two functions $F^{(a_k)}(z)$ are known and they are of the form ($a_{k,j}$ are known):

$$F^{(a_k)}(z)=1+2z, \quad \text{for } k\text{=1 or 2.} \qquad (24)$$

which means that $N_p=1$. For the general model problem, polynomials $F^{(a_k)}(z)$ are not known.

With the SFBIM, the solution of the model problems analyzed is approximated by the leading N_a terms of the local asymptotic expansion (21):

$$\overline{\Phi}(r,\theta,z) = \sum_{k=1}^{N_a} \left\{ \sum_{j=1}^{N_p+1} a_{k,j} \underbrace{\left[z^{j-1} + \sum_{i=1}^{N} c_{k,i} \partial_z^{2i}\left(z^{j-1}\right) r^{2i} \right] r^{a_k} \sin\left(a_k(\theta - \varphi_A)\right)}_{V_k^{(j)}} \right\} \quad (25)$$

where the over-bar denotes an approximate quantity. In the above expansion, the inner function, denoted by $V_k^{(j)}$, is the so-called singular function, in which N is an additional parameter, selected so that N_p<2N+1, the latter being the result of the substitution of Φ, expressed by (25), into the governing equation (Elliotis 2016) and asking the expression to satisfy the 3-D Laplace equation. Also, parameter $c_{k,i}$ is defined as $c_{k,i} = (-1/4)^i / \left(\Pi_{l=1}^{i} l(\alpha_k + l)\right)$.

Following the standard procedure of the SFBIM for the 3-D case (Christodoulou et al. 2012b, Elliotis et al. 2010, Elliotis 2016), the governing equation is weighted by the singular functions $V_k^{(j)}$, in the Galerkin sense, to give $(N_p+1)N_a+N_\lambda$ discretized equations. Then, after applying Gauss divergence theorem and by considering that functions $V_k^{(j)}$ satisfy exactly the boundary conditions along S_A and S_B and also by imposing the Dirichlet boundary condition on S_C, by means of Lagrange multiplier $\mu(\theta,z)$, we finally arrive at the following linear system of $(N_p+1)N_a+N_\lambda$ discretized equations:

$$\iint_{S_C} \left(\mu V_k^{(j)} - \overline{\Phi}\left(\partial_n V_k^{(j)}\right)\right) dS + \iint_{S_D} \left(-\zeta V_k^{(j)} + \overline{\Phi}\left(\partial_n V_k^{(j)}\right)\right) dS + $$
$$+ \iint_{S_E} \left(\zeta V_k^{(j)} - \overline{\Phi}\left(\partial_n V_k^{(j)}\right)\right) dS = 0, \quad (26)$$
$$k = 1,2,\cdots,N_a, \qquad j = 1,2,\cdots,N_p+1$$

$$\iint_{S_C} \overline{\Phi} B_i \, dS = \iint_{S_C} q_s(\theta,z) B_i \, dS, \qquad i = 1,2,\cdots,N_\lambda \quad (27)$$

In applying the SFBIM for the general model problem, equation (27) takes the form:

$$\iint_{S_C} \overline{\Phi} B_i \, dS = \iint_{S_C} p_g(\theta,z) B_i \, dS, \qquad i = 1,2,\cdots,N_\lambda \quad (28)$$

In (26) Lagrange multiplier $\mu(\theta,z)$ is expanded in terms of bilinear basis functions $B_i(\theta,z)$:

$$\mu(\theta,z) = \partial_n \overline{\Phi}(r,\theta,z) = \sum_{i=1}^{N_\lambda} \mu^{(i)} B_i(\theta,z), \quad \text{with } r=R \text{ on } S_C \quad (29)$$

As in previous applications of the method, the nodal values of μ are the additional unknowns.

System of Discretized Linear Equations in Block Form

Integration is performed away from the boundary singularity *OD* which lies along the *z*-axis. This is an advantage for the procedure since the *z*-axis is a strong singularity. Furthermore, the system of discretized equations (26) and (27) or (28) is a system of linear equations in which $\Phi(r,\theta,z)$ and $\mu(\theta,z)$ are substituted by their expansions (25) and (29), respectively.

The coefficients of the unknowns $a_{k,j}$ and $\mu^{(i)}$ are represented by expressions with integrals which contain terms with $V_k^{(j)}$ and $B_i(\theta,z)$ and their derivatives. The system takes the form:

$$\begin{bmatrix} M_1 & M_2 \\ M_2^T & M_0 \end{bmatrix} \cdot \begin{bmatrix} \mathrm{X} \\ \Lambda \end{bmatrix} = \begin{bmatrix} C_0 \\ C_C \end{bmatrix} \qquad (30)$$

where vector X contains the first set of unknowns $a_{k,j}$ and vector Λ contains the second set of unknowns $\mu^{(i)}$. Sub-matrix M_0 and vector C_0 contain zeros. System (30) is solved by using the Gauss elimination procedure. Obviously, the stiffness matrix is symmetric and it becomes singular or ill-conditioned (Xenophontos et al. 2006) when $(N_p+1)N_a<N_\lambda$ in which case the method diverges.

Numerical Results

For the estimation of integrals (26), (27) and (28) for both the general and specific model problems, numerical integration takes place on all boundary parts, except from S_A and S_B. For example, the calculation of integrals on S_C is performed by applying $N_E=N_z\times N_\theta$ boundary elements on this boundary part. Integration takes place on each element by using a 3×3 Gauss-Legendre quadrature rule. The boundary elements grid and the shape of basis functions are presented in Figure 6.

Figure 6. *Grid of Boundary Elements and Shape of Basis Functions*

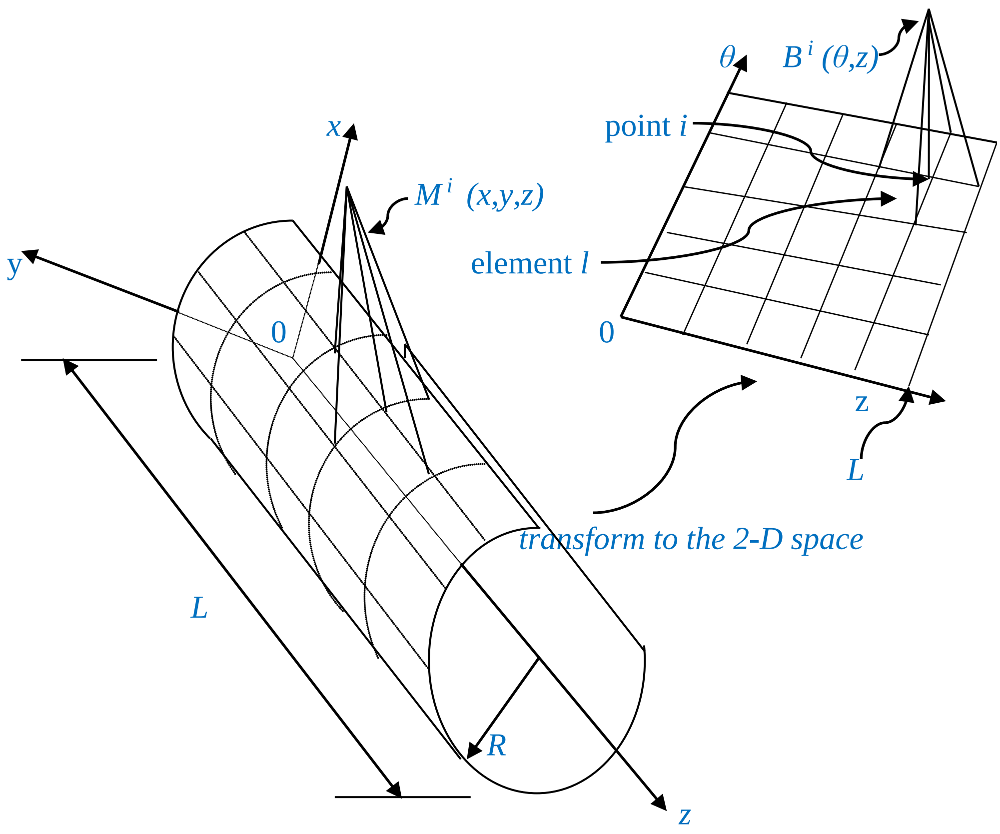

Table 1 presents the converged values of the leading singular coefficients $a_{k,j}$ corresponding to the general model problem obtained with both the SFBIM and the FEM, for a specific value of d_c (distance between the edge singularity and the z-axis as indicated in Figure 5) and for a specific value of small axis b (see the elliptic cross-section in Figure 3). Thus, as the value of the big axis a, on the elliptic cross-section, varies, different values of singular coefficients are obtained at convergence in using the SFBIM. It must be noted that with the method, convergence occurs for a specific combination of $(N_p+1)N_a$, in number, singular coefficients and of N_λ Lagrange multipliers. Also, the CPU time has been recorded for both the SFBIM and the FEM. One may easily observe that the SFBIM is much more accurate and much faster than the FEM.

Table 1. *Converged Values of the Leading Singular Coefficients $a_{k,j}$ of the General Model Problem, Obtained with the SFBIM and the FEM for d_c=0.6 cm and b=1.5 cm*

L (cm)	*a/b*	ω_d *(rads)*	*Leading singular coefficients* $a_{k,j}$ *k*	*j*	**SFBIM** average CPU time per run = 0.6 sec	**FEM** (with grid refinement) average CPU time per run= 22.7 sec
			1	1	1.0000000000000012	1.0004
		0.1998π	1	2	2.0000000000000014	1.9997
		:	2	1	1.0000000000000013	0.9995
		:	2	2	1.9999999999999985	2.0003
	1.20		:	:	:	:
			:	:	:	:
		:	1	1	1.0000000000000057	0.9996
		1.9998π	1	2	1.9999999999999949	2.0002
0.1			2	1	1.0000000000000062	1.0004
	:	:	2	2	2.0000000000000077	2.0002
		:	:	:	:	:
	:		:	:	:	:
		:	1	1	1.0000000000000059	0.9997
	3.00		1	2	2.0000000000000073	2.0001
		1.9998π	2	1	1.0000000000000081	1.0003
			2	2	2.0000000000000064	2.0001
:	:	:	:	:	:	:
:	:	:	:	:	:	:
4.0		:	1	1	1.0000000000000069	1.0003
	3.00	:	1	2	2.0000000000000057	2.0002
		1.9998π	2	1	1.0000000000000074	1.0001
			2	2	2.0000000000000087	2.0001

Table 2 contains the converged values of the leading singular coefficients $a_{k,j}$ corresponding to the specific model problem, for a radius *R* of the rivet equal to 1 cm and for the case where the edge singularity coincides with the *z*-axis. These numerical results (converged values) were obtained by the SFBIM and for the "optimal" combination of the number of singular coefficients and Lagrange multipliers. Also, it is observed that the numerical error with the SFBIM is significantly less than the error which occurs in using the FEM. With Table 3 a comparison is made between the two methods for the values of the polynomial functions at *z*=1.0, regarding the specific model problem. Again, one may easily see how much faster and accurate is the SFBIM compared with the FEM employed together with grid refinement.

Table 2. *Converged Values of the Leading Singular Coefficients $a_{i,k}$, Regarding the Specific Model Problem, for R=1cm and for d_c=0 cm, with the SFBIM and the FEM*

k	j	$a_{k,j}^{(SFBIM)}$ (for "optimal" combination $(N_p+1)N_a=32$; $N_\lambda=16$; $N_p=3$; $N=2$)	$a_{k,j}^{(FEM)}$ (with grid refinement)	$a_{k,j}^{(exact)}$	*error with the SFBIM* $\lvert a_{k,j}^{(SFBIM)} - a_{k,j}^{(exact)}\rvert$ average CPU time per run = 0.4 sec	*error with the FEM* $\lvert a_{k,j}^{(FEM)} - a_{k,j}^{(exact)}\rvert$ average CPU time per run = 17.2 sec
1	1	1.0000000000000016	1.0003	1.0000	1.6×10^{-15}	3×10^{-4}
1	2	2.0000000000000021	1.9999	2.0000	2.1×10^{-15}	1×10^{-4}
2	1	1.0000000000000018	0.9997	1.0000	1.8×10^{-15}	3×10^{-4}
2	2	2.0000000000000031	2.0002	2.0000	3.1×10^{-15}	2×10^{-4}

Table 3. *Comparison Between the Exact Solution and the Values Obtained by the SFBIM and the FEM, for R=1, d_c=0 cm and z=1.0 cm, for the First Two Polynomial Functions $F^{(a_k))}(z)$ Regarding the Specific Model Problem*

k	$F_{SFBIM}^{(a_k)}$	$F_{FEM}^{(a_k)}$	$F_{exact}^{(a_k)}$	$\left\lvert F_{SFBIM}^{(ak)} - F_{exact}^{(a_k)}\right\rvert$	$\left\lvert F_{FEM}^{(ak)} - F_{exact}^{(a_k)}\right\rvert$
1	3.0000000000000037	3.0002	3.0000	3.7×10^{-15}	2×10^{-4}
2	3.0000000000000049	2.9999	3.0000	4.9×10^{-15}	1×10^{-4}

The efficiency of the method is depicted in the graph shown in Figure 7 where error is defined as

$$\varepsilon_k = \left| F^{(a_k)}(z) - \overline{F}^{(a_k)}(z) \right|_{z=1} \qquad k = 1 \text{ or } 2 \tag{31}$$

where $\lvert . \rvert_{z=1}$ is the absolute value of the difference between the exact and the approximate values of $F^{(a_k)}(z)$ at z=1, for d_c=0 and ω=1.9998π *rads*. Graph indicates very high accuracy and fast convergence of the SFBIM.

Figure 7. *Graph of Errors ε_1 and ε_2 for $F^{(a_1)}$ (Lower Line) and $F^{(a_2)}$ (Upper Line) at z=1*

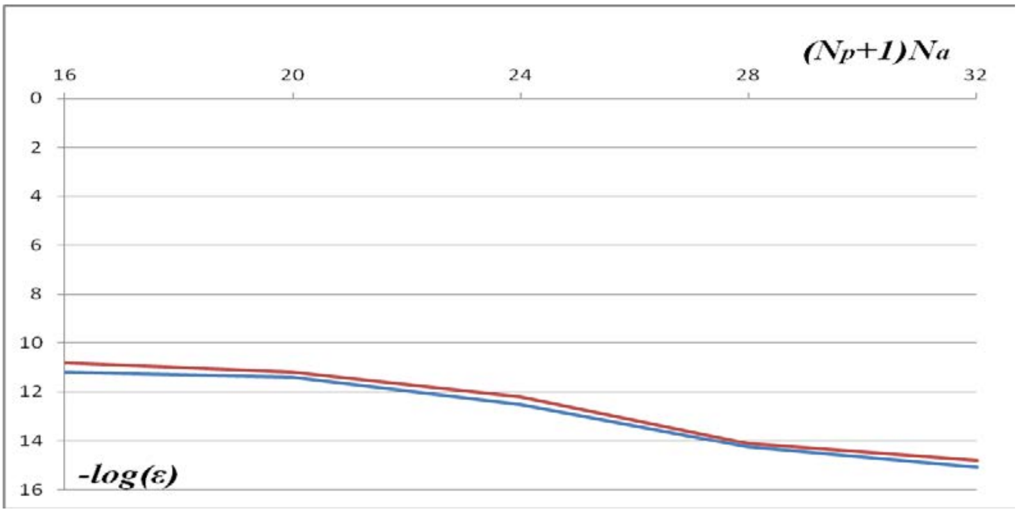

Having the numerical approximations of the singular coefficients, for the specific problem, the approximate function $\Phi_s(r,\theta,z)$ of the solution is now in complete form and the stresses at any point of the solid body (domain Ω_s with $d_c=0$ and thus $\omega_d=\omega$) at Figure 5, can be calculated from the following expressions in cylindrical coordinates (remember that eigen-values are $a_k=((2k\text{-}1)\pi)/(2\omega)$), in which index s is dropped:

$$\sigma_{rr} = \partial_r^2 \overline{\Phi} \approx (1+2z)\sum_{k=1}^{2}\left[a_k(a_k-1)r^{a_k-2}\sin(a_k\theta)\right] \quad (32)$$

$$\sigma_{\theta\theta} = r^{-1}\partial_r\overline{\Phi} + r^{-2}\partial_\theta^2\overline{\Phi} \approx -(1+2z)\sum_{k=1}^{2}\left[a_k(a_k-1)r^{a_k-2}\sin(a_k\theta)\right] \quad (33)$$

$$\sigma_{zz} = \partial_z^2\overline{\Phi} \approx 0 \quad (34)$$

Note that in considering the series expansion of the above stresses it is always $\sigma_{rr}+\sigma_{\theta\theta}+\sigma_{zz}=0$ in all over domain Ω. This result is also deduced by adding stresses σ_{rr}, $\sigma_{\theta\theta}$, σ_{zz} which are expressed in terms of the potential. Also, the shear stresses are given by

$$\sigma_{r\theta} = \partial_r\left(r^{-1}\partial_\theta\overline{\Phi}\right) \approx (1+2z)\sum_{k=1}^{2}\left[a_k(a_k-1)r^{a_k-2}\cos(a_k\theta)\right] \quad (35)$$

$$\sigma_{\theta z} = r^{-1}\partial_{z,\theta}^2\overline{\Phi} \approx 2\sum_{k=1}^{2}\left[a_k r^{a_k-1}\cos(a_k\theta)\right] \quad (36)$$

$$\sigma_{zr} = \partial_{z,r}^2\overline{\Phi} \approx 2\sum_{k=1}^{2}\left[a_k r^{a_k-1}\sin(a_k\theta)\right] \quad (37)$$

Table 4. *Values of Stresses at Position z=2 cm, with d_c=0 r=0.01 cm, at θ≈0 and θ≈ω*

Type of stress *(MPa)*	$\theta \to 0$	$\theta \to \omega$
σ_{rr}	0	-26.68
$\sigma_{\theta\theta}$	0	26.68
σ_{zz}	0	0
$\sigma_{r\theta}$	-32.58	0
σ_{rz}	0	0.11
$\sigma_{\theta z}$	0.21	0

Using the above expressions, the values for the stresses are obtained at z=2 cm, for θ=0 and for θ=ω, respectively, very near to the edge-singularity (r=0.01 *cm*) of problem's domain Ω_s. Position z=2 cm is chosen to have the greatest absolute values for all components of the stress tensor. These values are tabulated in Table 4.

Note that according to the theory of fracture Mechanics the mean value of the only out of plane displacement ξ_z and the values of stresses $\sigma_{\theta z}$ at $\theta \approx 0$ and σ_{rz} at $\theta \approx \omega$ are important for us since they help to arrive at the conclusion that the crack of the specific model problem (Figure 5) is of Mode III. Then one needs to calculate the Mode III FMP which is denoted by K_{III}. Stresses $\sigma_{\theta z}$ and σ_{rz} at $\theta \approx 0$ and $\theta \approx \omega$, respectively, are acting in the same direction but because $|\sigma_{\theta z}| \neq |\sigma_{rz}|$ there is a differential displacement between the two parts, on the left and on the right of the V-notch, along the length of the solid body. Thus, the crack is of Mode III. Parameter K_{III} is then calculated from (Aliabadi and Rooke 1991):

$$K_{III} = \lim_{r \to 0} \left(\sqrt{2\pi r}\, \sigma_{\theta z} \Big|_{\theta = \frac{\omega}{2},\ z=2} \right) \qquad MPa.m^{1/2} \tag{38}$$

Table 5 presents the values of $\sigma_{\theta z}$ in *MPa* and of K_{III} in $MPa.m^{1/2}$, with respect to r, calculated at the position with z=2 cm and θ=ω/2 and rounded to the 3rd decimal digit, as it is the custom in engineering applications. Also, Figure 8 depicts the behavior of K_{III} as r decreases. Since the material of the solid body of this problem is a high yield steel with a value of critical parameter $K_{III,c}$=50 $MPa.m^{1/2}$, then the largest of the values of K_{III}, which is obtained for the "nano-dimension" $r=10^{-7}$ cm (Table 5) indicates that there is no danger of crack propagation for the specific problem (i.e., $K_{III,max} < K_{III,c}$).

Table 5. *Values of the Stress Intensity Factor K_{III} for d_c=0 and for Different Values of r at z=2 cm and θ=ω/2*

r (*cm*)	$\sigma_{\theta z}$ (*MPa*)	*Mode III FMP* K_{III} ($MPa.m^{1/2}$)
10^{-2}	0.078	0.002
10^{-3}	0.570	0.005
10^{-4}	3.430	0.009
10^{-5}	19.657	0.016
10^{-6}	111.198	0.028
10^{-7}	626.230 (first yield)	0.049

Yielding (i.e., plastic deformation) does not take place anywhere in the material of the rivet, except from the area around the tip of the crack and within a cylindrical region of the material of radius $r=10^{-5}$ *cm*, in which plastic deformations and plastic strains (Fung 1977) take place (stress state exceeds the elastic limit but is confined within the plastic region which is formed around the singularity). Consequently, the solid body does not fail under the stress state and stress concentration in the region of the straight-edge singularity.

Figure 8. *Graphical Representation of Mode III Fracture Mechanics Parameter K_{III} for $d_c=0$ and at $z=2$ cm, $\theta=\omega/2$*

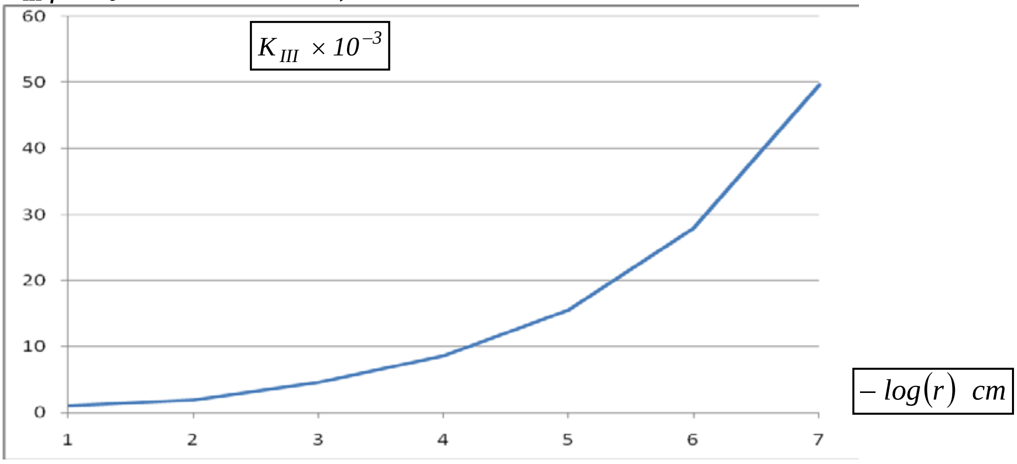

Conclusions

In this study two 3-D model problems are tackled. These are problems of linear elasticity in fracture Mechanics which are reduced to elliptic boundary value problems with a Laplacian governing equation of a Lamé potential. The first problem is a general model problem of a cylindrical body with a cross section in the form of an ellipse which retains its shape along the *z*-axis. The second model problem is a specific problem of a steel rivet (it could be also a steel bolt), with a circular cross section, which connects three elements of a structure. Both problems have a surface V-notch with a vertex which is treated as a boundary singularity.

The SFBIM, which is a Trefftz method, has been implemented in the current study and as in other previous applications of the method, very fast convergence and very high accuracy are achieved, in directly calculating the singular coefficients of the local solution expansion. Comparison between the results obtained for the values of the singular coefficients $a_{k,j}$ and the polynomial functions $F^{(a_k)}(z)$, with the SFBIM and the FEM (with grid refinement), shows that the latter is not as efficient as the SFBIM. Indeed, the numerical results indicate that our method presents much greater accuracy and much smaller computational time (smaller CPU time on the same computing machine) in compare to the FEM. The greater accuracy achieved by the method, is demonstrated by comparing the results of the two methods which were obtained in solving both the above general model problem (in which the exact solution is not available) and the above specific model problem with a known solution. In fact, for both model problems, in implementing the SFBIM the mean value of the numerical error, at convergence, in all runs, is of the order of 10^{-15}, while for the FEM the corresponding error is about 10^{-4}.

Especially for the specific model problem, the results are also compared with the exact solution. Thus, the extension of this technique to both the general and the specific model problems is quite interesting, from the engineering point of view, since it constitutes a novel application of this specific methodology of applied mathematics in engineering. In particular, the capability of the method to tackle problems of Fracture Mechanics with crack discontinuities (boundary singularities) more efficiently and effectively in compare to the FEM with grid refinement, is demonstrated with the current study, something which encourages the implementation of its algorithm in subroutines of engineering packages to solve specific problems with boundary singularities, a domain in which other numerical schemes extract the values of the singular coefficients by post-processing the numerical solution.

As a general remark we would say that the application of the SFBIM to solve the above model problems, encourages its extension to other engineering problems with boundary singularities of a different type and with more complicated geometry and boundary conditions.

References

Aliabadi M, Rooke D (1991) *Numerical fracture mechanics*. United Kingdom: Kluer Academic Publishers.

Bernal F, Kindelan M (2010) Radial basis function solution of the Motz problem. *Engineering Comput*ations 27(Jul): 606–620.

Brannick JJ, Li H, Zikatanov LT (2008) Uniform convergence of the multi-grid V-cycle on graded meshes for corner singularities. *Numerical Linear Algebra with Applications* 15(2–3): 291–306.

Brenner SC (1999) Multigrid methods for the computation of singular solutions and stress intensity factors I: corner singularities. *Mathematics of Computation* 68(226): 559–583.

Brenner SC, Scott LR (1994) *The mathematical theory of finite element methods*. New York: Springer.

Chaumont-Frelet T and Nicaise S (2018) High-frequency behaviour of corner singularities in Helmholtz problems. *ESAIM: Mathematical Modelling and Numerical Analysis* 52(5): 1803–1845.

Christodoulou E, Elliotis M, Xenophontos C, Georgiou G (2012a) Analysis of the singular function boundary integral method for a biharmonic problem with one boundary singularity. *Numerical Methods for Partial Differential Equations* 28(3): 749–767.

Christodoulou E, Elliotis M, Xenophontos C, Georgiou G (2012b) The singular function boundary integral method for 3-D Laplacian problems, with a boundary straight-edge singularity. *Applied Mathematics and Computation* 219(3): 1073–1081.

Costabel M, Dauge M, Duduchava R (2003) Asymptotics without logarithmic terms for crack problems. *Communications in Partial Differential Equations* 28(5–6): 869–926.

Dauge M and Nicaise S (2017) Special issue: singularities, integral equations and electromagnetism preface. *Mathematical Method in the Applied Sciences* 40(2): 328–338.

Elliotis M, Christodoulou E, Georgiou G, Xenophontos C (2010) *the singular function boundary integral method for a 3-D Laplacian problem with an edge singularity*. Recent Development in Boundary Element Methods (a volume to honour John T Katsikadelis). WIT Press.

Elliotis M, Georgiou G, Xenophontos C (2002) The solution of Laplacian problems over L-shaped domains with a singular function boundary integral method. *Communications in Numerical Methods in Engineering* 18(3): 213–222.

Elliotis M, Georgiou G, Xenophontos C (2005a) Solution of the planar Newtonian stick-slip problem with a singular function boundary integral method. *International Journal for Numerical Methods in Fluids* 48(9): 1000–1021.

Elliotis M, Georgiou G, Xenophontos C (2005b) Solving Laplacian problems with boundary singularities: a comparison of a singular function boundary integral method with the p/hp version of the finite element method. *Applied Mathematics and Computation* 169(1): 485–499.

Elliotis M, Georgiou G, Xenophontos C (2006) The singular function boundary integral method for a two-dimensional fracture problem. *Engineering Analysis with Boundary Elements* 30(2): 100–106.

Elliotis M, Georgiou G, Xenophontos C (2007) The singular function boundary integral method for biharmonic problems with crack singularities. *Engineering Analysis with Boundary Elements* 31(3): 209–215.

Elliotis M, Charmpis D, Georgiou G (2014) The singular function boundary integral method for an elastic plane stress wedge beam problem with a point boundary singularity. *Applied Mathematics and Computation* 248(Dec): 93–100.

Elliotis M (2016) The singular function boundary integral method for the 2-D and 3-D Laplace equation problems in mechanics, with a boundary singularity. *Pure and Applied Mathematics Journal* 5(6): 192–204.

Elliotis M (2019) A mathematical model for a steady-state seepage flow of groundwater under a reinforced concrete dam. *Applied Computing and Geosciences* 1(Oct): 100003.

Fung YC (1977) *Foundations of solid mechanics*. New Jersey: Prentice-Hall Inc.

Georgiou GC, Olson L, Smyrlis G (1996) A singular function boundary integral method for the Laplace equation. *Communications in Numerical Methods in Engineering* 12: 127–134.

Karageorghis A (1992) Modified methods of fundamental solutions for harmonic and biharmonic problems with boundary singularities. *Numerical Methods for Partial Differential Equations* 8(1): 1–19.

Katsikadelis J (1991) Large deflections of plates on elastic foundation by the boundary element method. *International Journal of Solids Structures* 27(15): 1867–1878.

Li ZC (1998) *Combined methods for elliptic equations with singularities, interfaces and infinities*. Boston: Kluer Academic Publications.

Li ZC, Lu TT, Huang HT, Cheng A (2007) Trefftz collocation and other boundary methods – A comparison. *Numerical Methods for Partial Differential Equations* 23(1): 93–144.

Li ZC, Lu TT, Hu HY, Cheng A (2008) *Trefftz collocation methods*. Southampton, Boston: WIT Press.

Omer N, Yosibash Z (2019) Extracting stochastic stress intensity factors using generalized polynomial chaos. *Engineering Fracture Mechanics* 206(Feb): 375–391.

Schapira Y, Yosibash Z (2020) Asymptotic solution of the elasticity equations in the vicinity of an elliptical crack front. *Engineering Fracture Mechanics* 223(Jan): 106774.

Seshaiyer P, Suri M (1998) Conforming results for non-conforming hp methods: the mortar finite element method. *Contemporary Mathematics* 218: 453–459.

Stephan E, Whiteman JR (1988) Singularities of the Laplacian at corners and edges of three-dimensional domains and their treatment with finite element methods. *Mathematical Methods in the Applied Sciences* 10(3): 339–350.

Szabo BA, Yosibash Z (1996) Numerical analysis of singularities in two dimensions Part 2: Computation of generalized flux/stress intensity factors. *International Journal for Numerical Methods in Engineering* 39(3): 409–434.

Woo G, Kim S (2018) Stress intensity factors and finite element solutions for corner singularities. *East Asian mathematical journal* 34(5): 623–632.

Xenophontos C, Elliotis M, Georgiou G (2006) The singular function boundary integral method for elliptic problems with singularities. *SIAM J. Sci. Comput*. 28: 517–532.

Yosibash Z, Mittelman B (2016) A 3-D failure initiation criterion from a sharp V-notch edge in elastic brittle structures. *European Journal of Mechanics - A/Solids* 60(Nov-Dec): 70–94.

Yosibash Z, Schapira Y (2021) Edge stress intensity functions along elliptic and part-elliptic 3-D cracks. *Engineering Fracture Mechanics* 245(Mar): 107477.

Athens Journal of Technology and Engineering - Volume 9, Issue 4, December 2022 – Pages 305-320

Environmentally Friendly Building Materials with Beneficial Potential for Indoor Air Quality

By Gabriela Adela Călătan[*] & Carmen Dico[±]

Following the obvious increasingly interest for environmental protection and pollution reduction, worldwide, there is a strong orientation for identification and use in buildings some materials that require low power consumption and to determine a pollution low level in all stages of their production and exploitation. These energy and environmental protection criteria can be met successfully by a combination of unburned masonry bodies made of clay, mixed with various other natural materials, and sheep wool thermal insulation mattresses. These construction elements have a beneficial influence on the air quality of the interior space, ensuring, through the permeability to water vapor, the regulation of the relative humidity of the air and, through ability to store thermal energy in warm periods and release it in the cold ones, a uniform temperature distribution inside and avoiding high temperature fluctuations between seasons. Based on the experimental research results, we can identify solutions for achieving a vernacular housing (resistance walls, partition walls, floors, plasters, water protection, thermal insulation and finishing) in terms of safety, comfort and current aesthetic criteria.

Keywords: *adobe bricks, clay, hemp fibers, straw, sheep wool*

Introduction

Today, more than half of the population lives in the city and we are consuming natural resources faster than ever before. We are, without a doubt, the most "inventive" and "powerful" living thing on the planet. We are so full of "success" that we have arrested the entire planet in our interest, and the consequences are almost uncontrollable.

Fortunately, globally, the field of construction from ecological, natural, local materials is on the rise. In many countries, governments encourage their use in construction, with local authorities being among the most important beneficiaries. In Romania, natural, ecological houses have started to become more and more known and more and more specialists are interested in this type of construction (Ciurileanu and Bucur Horvath 2011).

One of the most commonly used vernacular materials is clay soil. It is suitable for making masonry bodies mixed with sand, lime, oils, natural resins, etc. The good behavior and satisfactory durability of constructions made of beaten clay and clay masonry bodies have been documented since the 19th century (Ciurileanu and Bucur Horvath 2011, Minke 2005). The clay is known as a material with adhesive properties in the fresh state, with mechanical strength in the hardened state and

[*]Senior Researcher, NIRD URBAN-INCERC Cluj-Napoca Branch, Romania.
[±]Senior Researcher, NIRD URBAN-INCERC Cluj-Napoca Branch, Romania.

even with waterproofing properties, after burned. Well-known are the old adobe houses covered with straw, the yurts of the nomadic peoples of the steppes of Central Asia heat-insulated with wool, special finishes made of bamboo, reeds or other fibers obtained from plant processing, all beautifully colored with paints obtained from fine grinding of some minerals, etc. Looking around us we easily find useful materials for each stage of the construction of a future house: structural material necessary for the construction of the foundation, walls, pillars, thermal insulation materials, waterproofing materials or noise insulation materials for pleasant-looking finishes. With a reduced financial, energy and labor effort, we can process these materials to be used to achieve a sustainable construction that meets the current needs of the user.

Another important property of clay is that it can be reused, obtaining very good results. The physical and mechanical performances of these newly manufactured bricks are not adversely affected by the use of recycled clay material. The paste obtained from the recycled clay material allows dispersed reinforcement by introducing vegetable fibers (straw or hemp fibers). These are well covered by the clay matrix, and after drying the specimens show physical-mechanical performance similar to those recorded when using freshly extracted clay.

By replacing, where possible, classical building materials with environmentally friendly materials, an important contribution is made to protecting the environment. The possibility of recycling, reuse, reintegration into nature, environmental protection and efficient management of natural resources are the basic indicators in the context of sustainable development. Thermal insulation construction materials made of unburned clay, wheat straw and sheep wool are successfully included in the category of ecological products (Minke 2005).

Another important quality of environmentally friendly materials is that they provide a healthy and pleasant climate for users. Clay-based building materials used in construction allow natural and efficient ventilation of the walls, water vapor permeability, thermal constancy and a constant humidity of the indoor environment. Also, these walls made of clay-based bricks have no toxic emissions, a factor that plays a very important role in reducing the risk of respiratory diseases, allergies and much more.

For thousands of years, sheep have been able to adapt to even the harshest of environments, as their wool protects them through hot, cold, damp and dry seasons. In this time, man has also used wool for this very protective property and for the many other benefits offered by the material. Because of their crimped nature, when wool fibres are packed together, they form millions of tiny air pockets which trap air, and in turn serves to keep warmth in during winter and out in the summer.[1]

Wool's unique advantage is its breathability. That is it's ability to absorb and release moisture from the surrounding air, without compromising it's thermal efficiency. When wool fibres absorbs moisture, they generate tiny amounts of heat. This warmth acts to prevent condensation in construction cavities by maintaining the temperature above the dew-point in damp conditions. This

[1] http://www.sheepwoolinsulation.ie/why_wool/default.asp.

property creates a natural buffering effect, stabilising heat changes that occur with relative humidity. Practically, this reduces the need to keep adjusting heating or cooling levels as wool insulation will keep a buildings cooler during the day and warmer during the night.[2]

Crimped wool fibres also gives the manufactured product particularly good resilience. This means that insulation made from wool will retain its thickness, one of the main contributors to insulation efficiency. As wool contains moisture, it is fire resistant, extinguishing itself when the source of flame is removed. It is also a very effective airborne and structureborne acoustic insulation, significantly reducing noises that can be heard throughout a building.

Being made from a naturally produced fibre, Sheep Wool Insulation requires less than 15% of the energy required to produce than glass fibre insulation. It can absorb and break down indoor air pollutants, such as formaldehyde, nitrogen dioxide and sulphur dioxide. Wool is a sustainable and renewable resource, that has zero ozone depletion potential and at the end of it's useful life can be remanufactured or biodegraded. Sheep wool insulation is safe and easy to handle and no protective clothing or special breathing apparatus is required to install it.[3]

Literature Review

Studies are presented in the literature that demonstrate the durability of constructions made with local materials and local techniques in different geographical and climatic conditions (Minke 2005).[4]

A major drawback of clay is that there is a high risk of cracking during drying due to significant axial shrinkage. The ideal clay soil, in order to be used in construction, must contain at least 15-16% clay, because it has the right plasticity and workability to obtain a quality finished product (Minke 2005, Bui, 2008, Kumar and Pushplata 2013, Ciurileanu and Bucur Horvath 2012). Thus, a linear contraction between 3 and 12% is accepted for bricks from soft mixtures or between 0.4 and 2% for drier mixtures (Moquin 1994). In order to obtain a good thermal insulation, the specialized literature indicates an apparent density of the material between 1,600 – 2,000 kg/m^3 (Bui, 2008, Kumar and Pushplata 2013, Ciurileanu and Bucur Horvath 2012, Moquin 1994).

In terms of mechanical strength, ASTM Code D1 633-00 New Mexico indicates a minimum compressive strength of the material required to make clay walls, of 2.07 N/mm^2. Zimbabwe's Code regarding the Clay Walls, requires for 400 mm thick and a single-level houses, a minimum compressive strength, of 1.5 N/mm^2 and of 2.0 N/mm^2 for two levels houses. The Australian standard indicates a compressive strength of at least 1.15 N/mm^2, and ASTM International E2392 /

[2] http://www.sheepwoolinsulation.ie/why_wool/default.asp.
[3] http://www.sheepwoolinsulation.ie/why_wool/default.asp.
[4] JournalSeek, getCITED, Google Scholar, Ideas-RePEc, IndexCopernicusTM, Intute, Israel Institute of Technology - Technion, Lupton Library, Munich Personal RePEc Archive, National Library of Australia, OPACPlus, Open J-Gate, ProQuest/Illustrata, ResearchGATE, Structurae, TIB/UB Hannover, UlrichswebTM, Universia, VUBIS, WorldCat®, WorldWideScience.org.

E2392M-10e1-2010 [6,7] indicates a value of 2,068 N/mm^2. ACI Material Journal Committee indicates values of compressive strength depending on the composition of the soil, as follows: 2.76 - 6.89 N/mm^2 for sandy soil, and 1.72 - 4.14 N/mm^2 for clay soil.

Currently there are some thermal insulation materials considered "classic" due to the high frequency of use. They are inorganic in nature (fiberglass wool or mineral wool) or organic in nature (expanded or extruded polystyrene, polyurethane foam) and account for about 87% of the market. "Alternative" thermal insulation materials represent only 13% of the market and include straw bales, hemp products, sheep wool, cotton wool, "smart" materials whose thermal insulation properties change dynamically depending on temperature (Bui et al. 2009, Kiroff and Roedel 2010).

Straw is an agricultural product. Compared to ordinary building materials, often used, neither their production, nor their use as a building material nor after demolition does not harm the environment or our health (Suciu and Suciu 2007).

Hemp is one of the first plants to be processed and used by humans over 12,000 years ago. Hemp is a variety of cannabis that is grown especially for fiber and seeds. It is one of the fastest growing plants in the world, with about 20 tons of dry produce per hectare each year. In addition, hemp is completely organic. Hemp has the highest industrialization capacity of all technical plants: nothing is thrown away, everything is capitalized. The hemp stalk from which the fibers are extracted is straight and has branches at the bottom. Its length is between 1 and 3 m, and the thickness varies from 4 to 8 mm. The anatomical tissues of the shell are more complex compared to flax. Among the many characteristics of hemp fiber are its superior hardness and durability and the amazing resistance to rot. In the composite form hemp is 2 times stronger than wood (Vural et al. 2007).

There are few references in the literature that show experimental results regarding the use of sheep wool as thermal insulation material. A synthesis of the studies carried out highlights the following characteristics and advantages: it is a natural insulating material, it has good thermal and sound-absorbing characteristics, even in the wet state, the most used fiber of animal origin; has the ability to store energy at high temperatures and transfer it to low temperatures; easily renewable, recyclable, with a low impact on the environment; beneficial to the health of the population by contributing to the preservation of the optimal indoor environment; retains its shape and volume due to the genetic structure of the threads which tend to always return to their original shape; it is a hygroscopic material (in conditions of normal humidity it absorbs water vapor up to 18%, and in conditions of high humidity until saturation, its humidity can reach up to 40%); it is a material that absorbs formaldehyde and other pollutants from the air (the products of wool's reaction with these substances are very stable products that are no longer released into the air); has a very good fire behavior, does not maintain combustion; does not contain toxic substances and has no radioactive emissions (Karim et al. 2011).

Over time, a number of criteria have been established to evaluate the quality of one thermal insulation material compared to another. In addition to thermal insulation performance, aspects of the impact on human health, from production to end of life, dust or fiber emissions, biopersistence, operational safety, environmental impact, fire behavior are currently being analyzed. , toxicity in case of fire and affordability in terms of price and method of purchase, installation and use.

Materials and Methods

The used raw materials, to make the experimental mixtures, were: clay, that was extracted from Valea Draganului, Cluj Napoca, Romania, wheat straw, hemp fibers and sheep flax.

The used sandy clay was characterized by particle size distribution (Figure 1) and oxide composition (Tables 1 and 2) (Asdrubali 2015).

Figure 1. *Sandy Clay Granulometry*

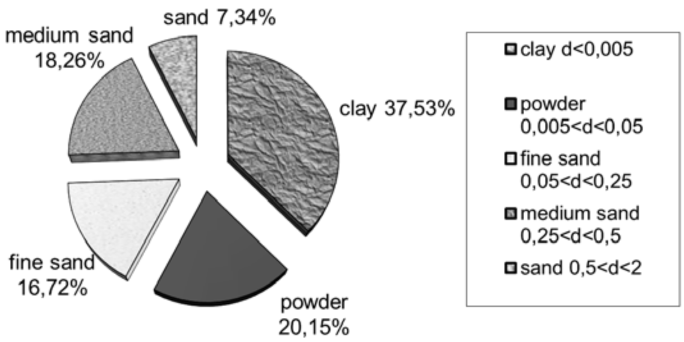

Table 1. *Clay Oxide Composition, Determined According to STAS 9163*

Oxides	SiO_2	Al_2O_3	Fe_2O_3	CaO	MgO	K_2O	Na_2O	TiO_2	PC
The content [%]	74.17	12.74	4.38	0.7	1.0	1.43	0.73	0.05	4.78

Table 2. *Oxidic Composition of Sandy Clay Used*

Identified oxide	SiO_2	Al_2O_3	Fe_2O_3	CaO	MgO	K_2O	Na_2O	TiO_2	PC
Concentration [%]	74.17	12.74	4.38	0.7	1.0	1.43	0.73	0.05	4.78

The sand used for the experimental research was characterized by an apparent density of 1,500 kg/m^3 and the granulometric distribution (Table 3).

Table 3. *Particle Size Distribution of the Sand Used*

Granulometric sieve size [mm]	0.063	0.125	0.25	0.5	1	2	4
Past [%]	0.5	1.6	8.8	28.5	59.6	82.4	98

The straws, having a high water absorption, were used after being previously immersed in water for one hour, in order to avoid the phenomenon of water absorption from the clay matrix.

Hemp fibers were purchased commercially and they were used as such.The hemp fibers was obtained from trade.

Plant materials were introduced into the clay matrix, expressed as a percentage by volume relative to the clay mixture (34% sand, 64% clay, 2% lime homogenized with 1.25% bone glue solution). Thus, 10% by volume of hemp fiber and 40% by volume of straw were introduced, respectively. The straw and fibers were cut to a length of about 7 cm. The bone glue was dissolved in warm water. From each mixture thus made, a set of 3 prismatic specimens, 40x40x160 mm, to determine the apparent density, axial shrinkage and mechanical strength and a set of 3 specimens of 300x300x40 mm, to determine the thermal conductivity were made. The specimens were kept in laboratory conditions until the equilibrium humidity was reached. The workability of the mixture during the preparation and manufacture of the test pieces was monitored (Călătan et al. 2016).

The thermal insulation material in sheep's wool comes from the Minet company, which managed to obtain a much more efficient thermal and acoustic, ecological insulation product made of natural wool fibers.

Sheep wool goes through certain stages of processing to the stage where it can be used as thermal insulation for homes. The wool is washed, mechanically combed and pressed into small layers. It is a non-woven product made by carding technology - folding from a mixture of recycled PET (polyethylene terephthalate), waste fibers PES (polyester) recycled, waste fibers, natural sheep wool fibers and vegetable fibers, cellulose and siliconized fibers, TENCEL®. In the final phase, after processing, the wool is brought in the form of thick and fluffy mattresses, condensed and with a shape similar to the basalt wool, used for insulation (Călătan et al. 2015, Abdou and Budaiwi 2013).

Figure 2.
a) Clay with Straw *b) Hemp Fiber Clay* *c) Sheep Wool Mattress*

Figure 3. *Wool-Based Composite Product*

The characteristics of the wool-based composite product were determined according to the standards for thermal insulation, by assimilation. The following tests were performed for 40mm thick wool mattress: bulk density, tensile strength perpendicular to the faces, short-term water absorption by partial immersion, long-term water absorption by total / partial immersion, tensile strength on longitudinal and transversal direction of the fabric, thermal conductivity, compressive strength.

In Figure 2, there are pictures of the clay mixture with straw (a), the clay mixture with hemp fibers (b) and the mattress made of sheep's wool.

Finally, a mixture was made for mortar, clay, sand, lime and bone glue (45.5% clay, 45.5% sand sort 0-2 mm, 9% hydraulic lime mixed with 3% bone glue solution) for plastering the wool mattress, Figure 3, and the appearance of cracks, adhesion resistance and water absorption on the plaster treated with linseed oil were followed (Adams 2017).

Results and Discussion

The tests were performed when the equilibrium humidity was reached, which was considered to be obtained after 40 days of storage of the specimens in laboratory conditions.

The clay biggest disadvantage is that it has a high shrinkage on drying, which causes cracks to appear on the surface of the products. When clay-based bricks are produced, they shrink when dried by reducing their size, so the brick obtained on drying will be smaller than the wet brick, but the finished product no longer has cracks, so it can be used as such, without the need for the addition of sand, that lowers the mechanical strengths.

When we want to get a plaster or clay masonry mortar, the contractions that produce cracks during drying are very important and and the aim is to reduce them (axial contractions). Drying cracking can be reduced by the addition of sand, which reduces shrinkage. The addition of sand will reduce the mechanical strength, but for a mortar this is not a problem. The most important properties of a masonry or plaster mortar are adhesion, in addition to water vapor permeability. For the plaster mortar applied to the outside, it is also necessary to improve the water resistance. Lime and/or dextrin are recommended to reduce the shrinkage of drying of a mortar and also to improve the resistance to erosion. Taking into account these recommendations resulting from previous studies, the clay-based mortar recipe, presented in the chapter Materials and methods, has been developed.

Also, for the significant improvement of the water resistance, the surface of the clay plaster was treated with linseed oil.

Analyzing the appearance of the clay specimens produced in accordance with the studied recept, at 40 days, it can be noticed the lack of surface cracks, which is a very important aspect for clay-based mixtures (Figure 4).

Figure 4. *Appearance of the Hardened Specimen Surface*

Table 4 shows the recipes made of clay, and Table 5 shows the results of the tests on the test pieces made on the basis of respective recipes.

Table 4. *The Made Recipes*

Recipe	A1	A2
Components added in mass percentages	34% sand, 64 % clay, 2 % homogenized lime with 1.25% bone glue solution	
Volume percentage	10% hemp fiber, 7 cm	40% straw, 7 cm

Table 5. *The Results Obtained*

Characteristic	A1	A2
Axial contractions [%]	6.1	3.4
Compressive strength [N/mm^2]	4.00	1.02
Bending strength [N/mm^2]	2.95	2.50
Density [kg/m^3]	1680	1383
Thermal conductivity [WmK]	0.38	0.17
Water vapor permeability μ	1.51	1.48

The results obtained on the nonwoven product made from a mixture of recycled PET (polyethylene terephthalate) waste fibers, recycled PES (polyester) waste fibers, natural sheep wool fibers and vegetable fibers, cellulose, siliconized, TENCEL® 40 mm thick, are shown in Table 6. The tests were performed in accordance with the European standards for thermal insulation.

The most important property of clay products is the permeability to water vapor. Water vapor permeability is a characteristic of porous materials that under the effect of molecular forces and of the imbalance between the external humidity of the environment and the humidity of the material allows diffusion through the material until an equilibrium is established. The diffusion rate through porous materials defines the vapor permeability coefficient. These products are vapor permeable which gives to the walls the property to breathe. The wall made with such products maintain a healthy and pleasant indoor environment.

Table 6. *The Obtained Results on the Sheep Mattress*

Characteristic		Value	Measurement Units
Apparent density		29.33	kg/m^3
Tensile strength perpendicular to the faces		1.3	kPa
Compressive strength	compaction at 0.12 kPa	7.2	%
	compaction at 0.25 kPa	16.7	
Tensile strength on the fabric longitudinal direction		0.05	N/mm^2
Elongation at tensile strength on the fabric longitudinal direction		23.48	%
Tensile strength on the fabric transverse direction		0.06	N/mm^2
Elongation at tensile strength on the fabric transverse direction		37.98	%
Short-term water absorption by partial immersion,Wp		0.191	kg/m^2
Long-term water absorption by partial immersion,Wlp		0.51	kg/m^2
Long-term water absorption by total immersion,Wh		12.91	%
Thermal conductivity coefficient		0.0358	W/mK
Water vapor permeability	W	11.30	m/m^{2}hPa
	μ	1.26	-

Following the results obtained, it can be stated that the thermal insulation product composite mattress based on sheep wool, is the best insulating material, with the lowest value of thermal conductivity. Straw clay has a good conductivity, but about 80% higher than sheep's wool. The advantage of clay materials over sheep linen is that they can be used as masonry bodies to make the walls, instead, the sheepskin mattress needs to be applied to an already built wall. Wool is also very sensitive to the action of mold and degradation in contact with the ground, it is not water resistant. A possible protection of the wool from mold and degradation could be the plaster, applied on its surface. For this purpose, a plaster based on clay, sand and lime was made. (45.5% clay, 45.5% sand sort 0-2 mm, 9% hydraulic lime mixed with 3% bone glue solution). The clay is also sensitive to water, but after applying 2 layers of linseed oil, it becomes waterproof (Suciu ανδ Suciu 2007). The first observation is that no cracks appear on the surface of the plaster, when drying, therefore, the tests were performed, the results of which are presented in Table 7.

Table 7. *The Test Results on the Test Specimen Made of Wool Plastered with a Clay Mixture and Treated with Linseed Oil*

Characteristic	Value	Measurement Units
Adhesion strength	1.30	kPa
Short-term water absorption by partial immersion,Wp	0.00	kg/m^2
Long-term water absorption by partial immersion,Wlp	0.01	kg/m^2

Discussion

Following the results obtained, it was found that the addition of straw to clay mixture, decreases the drying shrinkage, so the appearance of cracks, increases the resistance to bending, decreases the thermal conductivity, instead decreases the resistance to compression. When adding hemp fibers, the mechanical strengths are higher than with the straw-added test tube, however, the thermal conductivity is higher.

Based on the experimental results presented, regarding the sheep wool mattress can be said to have good performance in terms of thermal insulation capacity, has low mechanical strength, has good capabilities in terms of influence on indoor air quality - very good water vapor permeability, is sensitive to the action of water.

Figure 5. *The Thermal Conductivity Values of the Studied Materials Compared to Those of Polystyrene*

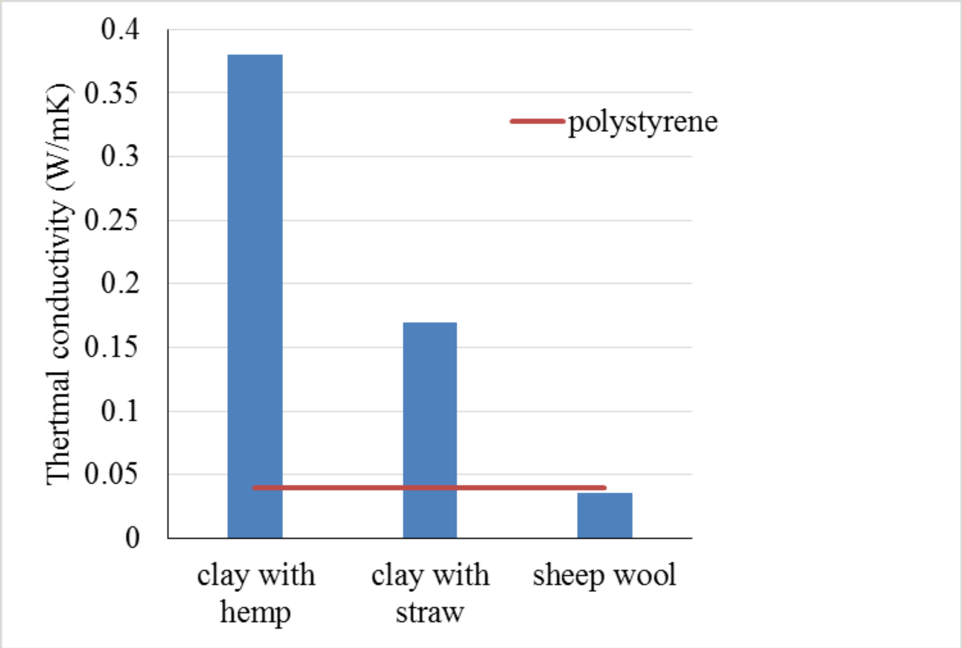

As shown in the graph in Figure 5, the composite mattress made of sheep wool is characterized by a lower coefficient of thermal conductivity than a polystyrene EPS 100.

The products obtained from clay have a higher thermal conductivity than polystyrene which has a higher thermal conductivit than the sheep's wool, so it can be concluded that the sheep's wool mattress is the best thermal insulation material, but it must be applied on a wall, already built.

Figure 6. *The Water Vapor Permeability Values of the Studied Materials*

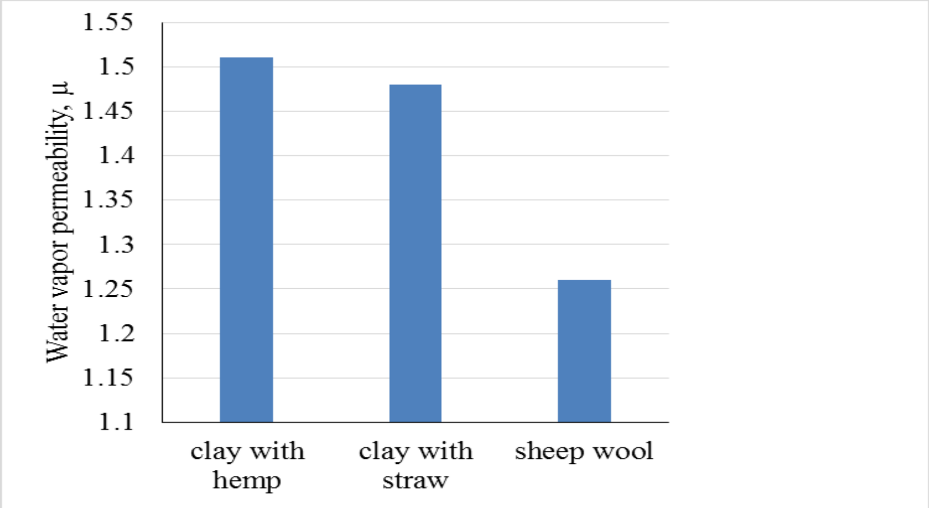

The graph in Figure 6 shows the values of the water vapor permeability coefficient of the product from hemp clay, straw clay and mixture of recycled PET (polyethylene terephthalate), waste fibers PES (polyester) recycled, waste fibers, natural sheep wool fibers and vegetable fibers, cellulose and siliconized fibers, TENCEL®. The higher is the permeability coefficient, the more waterproof the product is. Polystyrene EPS 100, has a vapor permeability coefficient of about 150. According to the graph, the studied products have a water vapor permeability coefficient in the range of 1.26-1.51, so it can be said that they are permeable to water vapor, which gives the wall, made of such materials, the property of breathing, while maintaining a constant humidity in the interior.

Following the results obtained on wool, it is observed that it is a thermal insulation material that has a lower coefficient of thermal conductivity than that of polystyrene, which means that it is a better thermal insulator than polystyrene. In addition, sheep's wool is also permeable to water vapor, and this means that water vapor diffuses through the linen layer. The problem with the linen mattress is that it must be applied to a wall that has already been made, due to poor mechanical strength of the mattress. In order for the wall to be completely breathable, it must be made of bricks made of materials with water vapor permeability such as clay, for example. Therefore, a solution would be for the wall, to be made of clay bricks, and for better insulation, to apply the linen mattress mixture of recycled PET (polyethylene terephthalate), waste fibers PES (polyester) recycled, waste fibers, natural sheep wool fibers and vegetable fibers, cellulose and siliconized fibers, TENCEL® and then, to continue to be plastered with a vapor-permeable clay-based mortar. To find out the compatibility between the linen mattress and the clay materials, it was treated with a clay-based plaster mortar, the recipe of which was indicated above. Following the results, it can be concluded that the adhesion of this plaster to wool is very good, also the water resistance is much improved, so it can be considered as an adequate method to protect the wool thermal insulation material. It is also an ecological and natural method, possible with local materials.

In conclusion, to obtain a wall, made of natural materials that have a good coefficient of permeability to water vapor, i.e., to be able to breathe, to have a low coefficient of thermal conductivity, i.e., to be a good thermal insulator and to have a good water resistance, materials based on clay, sheep's wool and linseed oil surface treatment can be used. The bricks from which the wall is made can be made of clay according to the studied recipes, then a layer of recycled PET (polyethylene terephthalate), waste fibers PES (polyester) recycled, waste fibers, natural sheep wool fibers and vegetable fibers, cellulose and siliconized fibers, TENCEL®. This mattress can be applied to the wall with the help of a studied clay-based mortar, and then plastered with clay mortar in 2 or 3 layers. For a good resistance to the action of climatic factors, the surface of the clay plaster on the outside is treated with 2 layers of linseed oil. The water resistance of flaxseed oil plaster has been previously studied and very good results have been obtained (Călătan et al. 2017). Figure 7 shows the results of water penetration tests under wind pressure, performed on various surface treatments in order to improve water resistance (Călătan et al. 2017). From the graph, it can be seen that the flaxseed oil treatment has the lowest water penetration coefficient under wind pressure, therefore it is the most effective treatment for improving the resistance to the action of climatic factors.

Figure 7. *Influence of the Surface Treatment on Water Penetration Coefficient under Wind Pressure (Călătan et al. 2017)*

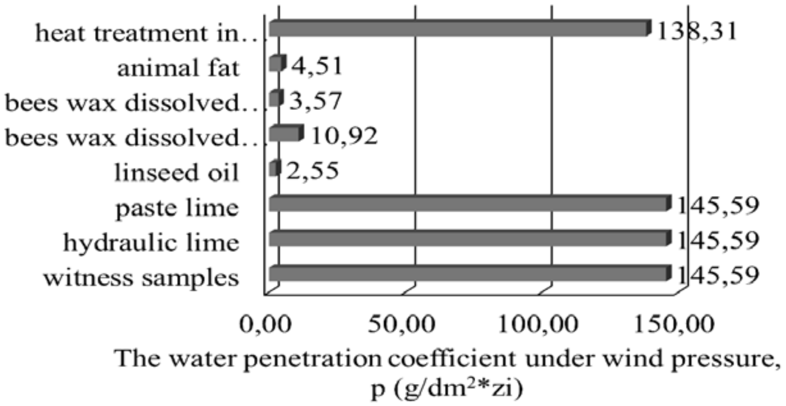

Conclusions

Following the study, the following conclusions can be drawn:

- Mixtures made of clay have a good workability, which allows a necessary homogenization.
- The value of the axial contractions is within the limit specified by the specialized literature, so that no clay mixture shows cracks when drying.

- The value of the density in hardened state of the clay mixture with the addition of hemp fibers is in the range 1,600 – 2,000 kg/m^3. According to the literature, this range is satisfactory in terms of thermal efficiency, which indicates a property of the wall made with such material, to keep a certain constant of the temperature of the indoor environment. The apparent density of the clay mixture with the addition of straw is below the lower limit of this range indicated by the literature, which means that this material, compared to the clay mixture with hemp fibers, has a lower capacity to store heat, on which, it can then give way when the temperature drops, instead it is a good thermal insulator.
- The products obtained from the two clay mixtures with the addition of hemp and straw, respectively, can be used to build a wall, due to the mechanical strength they have.
- Wool insulation material - has very good performance in terms of thermal insulation capacity, but has low mechanical strength, is sensitive to the action of water, is very sensitive to the action of mold and degradation in contact with the ground.
- Wool protection can be achieved by plastering its surface with a suitable plaster mortar, based on clay.
- Due to the fact that the clay material is also sensitive to the action of water, the surface of the clay plaster must be treated with a waterproofing solution, and previous studies show that the best solution for protection of clay plaster is the treatment with natural linseed oil.
- A combination of the two materials, the clay mixture and sheep's wool presents a suitable solution for creating an ecological, natural wall that gives a pleasant and healthy indoor climate.

The bricks made according to the recipes made of clay material studied can be used successfully to make the walls of buildings, and the insulation can be done with wool mattresses plastered and then with a clay-based mortar, and finally the surface is treated with linseed oil. A wall made in this way has good capacities in terms of influence on indoor air quality, very good permeability to water vapor, ability to absorb/desorb moisture from and into the environment, environmentally friendly, energy efficient and conferring a pleasant and healthy climate for inhabitants. At the same time, the basic principles of traditional vernacular architecture, which are modeled in accordance with current technological progress, are preserved.

Acknowledgments

This paper was financially supported by the Project "Entrepreneurial competences and excellence research in doctoral and postdoctoral programs - "ANTREDOC", project co-funded by the European Social Fund financing agreement no. 56437/ 24.07.2019."

Partial support was received from The Ministry of Research, Innovation and Digitalization (MCID) through the project PN 19 33 03 01, "Researches to achieve the acoustic and thermal comfort inside the buildings, using an innovative tool for choosing the optimum structures of construction elements, from classical versus modern materials".

References

Abdou A, Budaiwi I (2013) The variation of thermal conductivity of fibrous insulationmaterials under different levels of moisture content. *Construction and Building Materials* 43(Jun): 533–544.

Adams T (2017) *Sound material – A compendium of sound absorbing materials for architecture and design*. Tyler Adams.

Asdrubali F, D'Alessandro F, Schiavoni S (2015) A review of unconventional sustainable building insulation materials. *Sustainable Materials and Technologies* 4(Jul): 1–17.

Bui Q (2008) Durability of rammed earth walls exposed for 20 years to natural weathering. *Building and Enviroment* 44(5): 9–12.

Bui Q, Morel JC, Hans S, Meunier S (2009) Compression behaviour of non-industrial materials in civil engineering by three scale experiments: the case of rammed earth. *Materials and Structures* 42(8): 1101–1116.

Călătan G, Hegyi A, Dico C, Mircea C (2015) Additives influence on the earth characteristics used in vernacular construction. *Ecoterra - Journal of Environmental Research and Protection* 12(1): 7–20.

Călătan G, Hegyi A, Dico C (2016) Adobe bricks constructions. past experience, the base of the contemporary buildings. In *Proceedings of the 16th International Multidisciplinary Scientific GeoConference & EXPO – SGEM 2016, Section Green Buildings Technologies and Materials*. 28 iunie - 7 iulie 2016, Albena, Bulgaria.

Călătan G, Hegyi A, Dico C, Mircea C (2017) Experimental research on the recyclability of the clay material used in the fabrication of adobe bricks type masonry units. *Procedia Engineering* 181: 363–369.

Ciurileanu GT, Bucur Horvath I (2011) *The new vernacular based architecture*. JAES, Section Civil Engineering and Installations.

Ciurileanu GT, Bucur Horvath I (2012) Modular building using rammed earth. *Acta Technica Napocensis: Civil Engineering & Architecture* 55(2): 173–181.

Karim MdR, Zain Muhammad FM, Jamil M, Lai Fook C, Islam MdN (2011) Use of wastes in construction industries as an energy saving approach. *Energy Procedia* 12: 915–919.

Kiroff L, Roedel H (2010) Sustainable construction technologies: earth buildings in New Zealand. In *Proceeding of Second Internatiol Conference of Sustenable Constructions Materials and Technologies*. Ancona, Italy.

Kumar A, Pushplata (2013) Vernacular practices: as a basis for formulating building regulations for hilly areas. *International Journal of Sustainable Built Environment* 2(2): 183-192.

Minke G (2005) *Building with earth. Design and technology of a sustainable architecture, Birkhäuser*. Publishers for Architecture Basel Berlin Boston.

Moquin M (1994) *Ancient solutions for future sustainability: building with adobe, rammed earth, and mud*.Tampa, Florida, USA.

Suciu MC, Suciu N (2007) Dezvoltarea sustenabila - Problema cheie a secolului XXI. (Sustainable development - The key issue of the 21st century). *Buletinul AGIR* 1: 124–125.

Vural N, Vural S, Engin N, Sumerkan MR (2007) Eastern Black Sea region. A sample of modular design in the vernacular architecture. *Building and Environment* 42(7): 2746–2761.

Athens Journal of Technology and Engineering - Volume 9, Issue 4, December 2022 – Pages 321-338

Measuring the Level of Technology in Moral Economics

By Zsófia Hajnal[*]

This theory-based paper attempts classifying and combining methods of orthodox and heterodox economics regarding the measurement of technology levels. The importance of measuring the level of technology is illustrated by technology being a key factor in several neoclassical models. However, just as for the concept of utility, traditional economics treats the level of technology as an abstract scientific construct, without attempts for an absolute quantification. This paper argues that through a systematic classification and various methods, starting- and end points, milestones and even units can be determined. Through surveying the literature, the paper identifies the existing options of measurement, and their shortcomings. Technology is looked at as a "stock", as opposed to the overrepresented "flow" nature. This gives space for the methods of constructing an absolute scale, and for the unique concept of the "steady-state technology". Distinctions are made between demand-side and supply-side measurement, as well as between historical and geometrical methods of constructing scales. The methods are illustrated, though not fully implemented, due to limitations in scale and scope. Finally, the paper shows how heterodox economic branches, such as the newly emerging moral economic school, allow for the demand-side measurement to a greater extent, given the adjusted economic axioms.

Keywords: *technology, demand side, historical method, geometrical method, moral economics*

Introduction

By definition, technology is "the application of scientific knowledge to the practical aims of human life or, as it is sometimes phrased, to the change and manipulation of the human environment" (Encyclopedia Britannica 2021). In a professional context though, "a safe definition of what technology is troubles scientists of all fields" (Perilla Jimenez 2019, p. 826). In economics, beyond the understanding of technology being a "social construct" (Perilla Jimenez 2019, p. 826), technology is generally seen as a part of an efficiency coefficient which usually includes engineering or design elements. Economic literature is more specific on technology when it comes to levels and frontiers. The distinction between invention and innovation, and their circumstances, sophisticates the techno-economic picture: "Invention can be connected to almost anyone; however, in the case of innovation, at all events there is a need for a company or for some kind of organization" (Hámori and Szabó 2016, p. 52, footnote 1).

[*]Doctoral Student, Doctoral School of International Relations and Political Science, Corvinus University of Budapest & Visiting Lecturer, Budapest Business School – University of Applied Sciences, Hungary.

By the level of technology, some scholars understand the extent to which technology is utilized by a population (Veiseh 2010, p. 211). An overall consensus – even on the economic technology concept itself –, is yet to be reached among economists from different backgrounds (such as mainstream and evolutionary) (Perilla Jimenez 2019, p. 825).

To approach the *level* of technology concept, it may be advisable to provide a definition for the concept of technological change as well: "an increase in the outputs possible with a given level of inputs through the processes of invention, innovation, and diffusion" (Seo 2017). This latter definition appears to be a step closer to economic application than the initial definitions given, yet, it is the static *level of technology* notion that needs to be conceptualised to a greater extent.

The level of technology influences the whole of the economy, from the smallest steps of production, up to the validity of ruling economic ideologies, and to the "tectonic" shifts of economic systems. Thus, the significance of the level of technology in the field of economics should not be underestimated, yet from its meagre representation as a factor, one could draw the conclusion that it is.

The Aim of this Study

Despite its significance, the level of technology in economics is underexplained. It is only minimally included in curriculae of basic economics subjects, in the form of – at best – two or three relatively marginal topics.

The level of technology as an economic factor (or at least: dimension) is not just underexplained – it is underexplored too: Not a single JSTOR item in the field of economics has the expression "level of technology" in their title, and only two on the website of ScienceDirect do, but both of those are industry-specific, not theoretical.[5] Easing the searches by removing quotation marks results in a handful of further, exclusively empirical works.

To bring the level of technology into the economic discourse more intensively is now timely, also for the reason of societies currently being at multiple technological brinks. Several of the technologies having been labelled as "frontier" ones (UNCTAD 2021, p. 17), such as artificial intelligence, blockchain and gene editing, carry – upon more active, and potentially combined implementations – further and greater potentials of revolutionising everyday life, as well as international power-balances.

In economic analyses, the level of technology should be an aspect to be controlled for. In other words, when comparing various (regional, country-level, etc.) economies throughout time and space, it should be possible to determine how much the (desirably – quantified) level of technology affects the other macroeconomic indicators.

Thus, the aim of this research is to open the door to alternative, potentially more allowing and promising ways of measuring the level of technology.

The research questions are the following:

---

[5] Searches conducted on January 8, 2022; at: https://www.jstor.org/;https://www.sciencedirect.com/.

RQ1: How can the level of technology be measured in an economic context, objectively?
RQ2: Why is moral economics a suitable branch to provide the framework for economic technology level measurement?

Limitations

One limitation of the paper that should be noted is the exclusion of details regarding the concrete nature or patterns of technology changes. When examining technological advancement, the emphasis is on the global pace of invention and innovation, and not technological diffusion throughout various geographies. (Although technological "followers" follow other patterns of the technological development process than "leaders" do, this paper will remain in the generalised, theoretical realm, and should thus be unaffected by the lack of the distinction.) Further, this paper does not distinguish between the various innovation types (product, process, organisational, etc.). The discourse is kept general from this perspective as well, and the focus is on examining the shifts between the technology levels from an economic perspective. Neither does the paper look into the causes, the underlying factors that contribute to innovation. Classification and nomenclature of historical technology levels – such as the ones that can be related to Kondratiew-waves (long-term business-cycles), or expressions such as "industrial capitalism" and "information capitalism" (Hámori and Szabó 2016, pp. 69–70) – also remain absent. All restrictions serve to keep a focus on the *level of technology* as an operational, quantifiable concept.

Hypotheses

The primary hypothesis is that the level of technology can be measured objectively through historical and geometrical methods.

Second, that the framework, a novel approach, is provided by the moral economic branch, due to the availability of adjusted axiom of finite and satiable needs therein.

Structure

Although economic technology level measurement – theoretically, explicitly – has little substantial body of literature to date, the paper will provide an overview of the types and attempts. To present and emphasize the relevance of seeing the level of technology through the economist's lens, the paper will explore the rather restricted micro- and macroeconomic applications, then move on to contemporary aspects and challenges, i.e., the shortcomings of contemporary technology level measurements in the field of economics, and finally, synthesise insights in the context of moral economics.

Measuring the Level of Technology in Micro- and Macroeconomics

In the classical education of microeconomics, it is only at two main points (throughout the entire semester) that the level of technology gets a role or mention.

The Production Possibility Frontier and the Production Function

One such point is at the topic of the production possibility frontier (PPF), depicted in Figure 1. In this economic model, which showcases the most effective production options when one has to distribute their resources between two products, the emphasis is on the resources and their allocation. However, the level of technology is implicitly included.

Figure 1. *The Production Possibility Frontier*

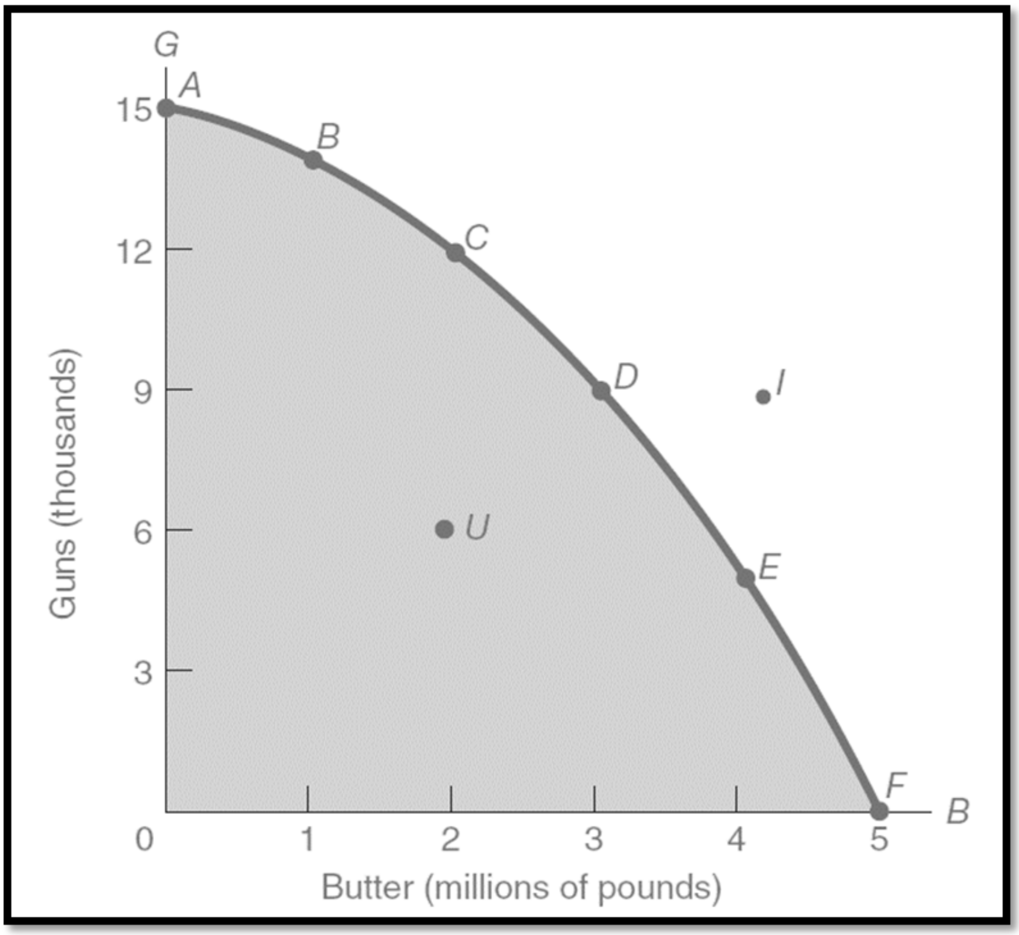

Source: Samuelson-Nordhaus (2010, p. 11).

The other microeconomic topic containing the level of technology, that has made its way into the classical study materials, is the production function (see Figure 2), specifying the maximum output that can be produced with a given quantity of inputs.

Figure 2. *The Production Function*

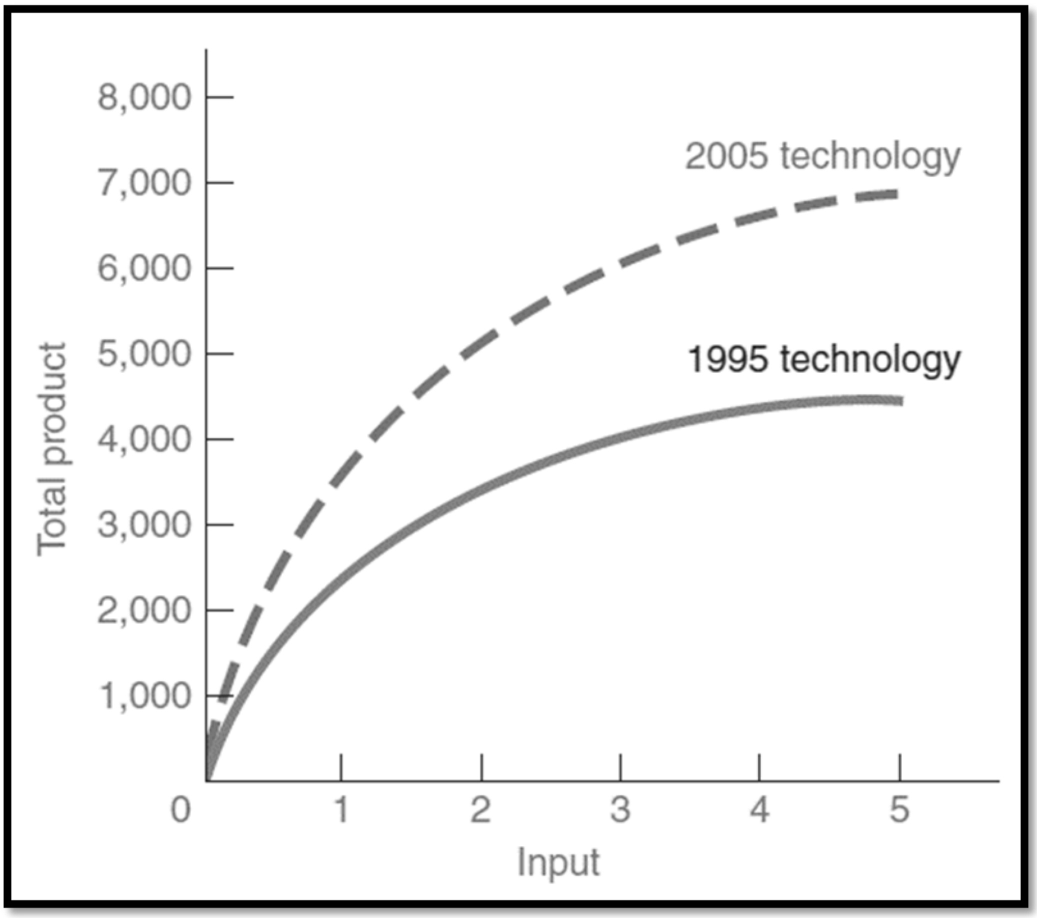

Source: Samuelson-Nordhaus (2010, p. 114).

This function then, is described with the Cobb-Douglas formula:

$$Y = A * L^{\alpha} * K^{\beta}$$

The letter Y stands for the total output, L and K for labour and capital inputs respectively, with the greek letters for the output elasticities, and – most importantly from this paper's perspective – A for the total-factor productivity (TFP), with the main, but not exclusive component of technology growth.

Endogenous Growth Theory

The next point in their studies, where an economic scholar-to-be learns about the level of technology, is upon hearing about the endogenous growth theory, which holds that "economic growth is an endogenous outcome of an economic system, not the result of forces that impinge from outside" (Romer 1994, p. 3). The endogenous growth theory belongs to the macroeconomic realm (Romer 1994, p. 10), and is distinguished from the neoclassical model of growth (Romer 1994, p. 3).

In contrast to the latter, which assumes "that technological change is exogenous and that the same technological opportunities are available in all countries of the world" (Romer 1994, p. 4), endogenous growth draws relationships between technology and input variables: A (K, L) (Romer 1994, p. 7).

This yields the following formula of a production function (Romer 1994, p. 7):

$$Y_j = A\,(K, L)\,K_j^{1-\alpha}\,L_j^{\alpha}$$

As Romer puts it bluntly: "Technological advance comes from things that people do" (Romer 1994, p. 12). His article, which the author of this essay has been citing so far, includes statements, on technology leaders and followers, knowledge diffusion, and the technology gap,[6] (Romer 1994, p. 9) as well as a direct mention in that context of the term "the level of technology"[7] (Romer 1994, pp. 4, 9).

Since the publishing of Romer's article, two generations of endogenous growth models have evolved. "First generation models (FGMs) are associated with the idea that technology leads to "persistent" and "increasing" rates of growth in the long-run. These models have been abandoned […] and replaced by second generation models (SGMs), a number of technically more appealing models that seek to explain what determines the observed empirical regularities of diminishing returns to technology investments." And even the SGMs have split since (Perilla Jimenez 2019, p. 830).

The reader can observe advances on the thinking of how and where technology changes, and on how to incorporate it as a factor in economics, but nothing substatially new arose on the measurement of its level, at this point.

As Perilla Jimenez notes: " […] even within mainstream economics—the nature of technology progress, its impact on economic growth and the role of public policy in this regard are not yet safely established" (Perilla Jimenez 2019, p. 831). It should be stated that the current paper does not focus on relating technology levels to economic growth and policy aspects, only on the measurement itself.

The Level of Technology – Contemporary Aspects

In this chapter, the paper will look at contemporary aspects and challenges, i.e., the shortcomings of contemporary technology level measurements in the field of economics, by investigating technology level roles in trade models, in trade statistics and in general trade dynamics. Empirical methods will be looked into as well, along with the possibilities of technology frontiers, in the context of innovation theory.

[6]"Because the flow of knowledge from the technology leader makes the technology grow faster in the follower country, income per capita will grow faster in the follower as diffusion closes what has been called a technology gap."

[7]"The assumption that the level of technology can be different in different regions is particularly attractive in the context of an analysis of the state data, because it removes the prediction of the closed-economy, identical-technology neoclassical model that the marginal productivity of capital can be many times larger in poorer regions than in rich regions."

In International Trade

The level of technology impacts the majority of trade models, but is relatively rarely mentioned explicitly. The articles that relate trade theory and technology levels directly are few and far between. The level of technology either only emerges in country case studies on trade (which typically provide an arbitrary scale for technology), or – less frequently – as an explanatory factor.

An example for this latter trend is Daniel Trefler's 1995 article *The Case of the Missing Trade and Other Mysteries*. Therein, Trefler finds the explanation for a generally poorly performing model (the Heckscher-Ohlin-Vanek theorem) in part in technology level differences between countries. Technology is quantified to some extent, but only in relative terms, for the purposes of the article.

Although there are plenty of statistics on scientific performance regarding trademarks, and in the form of R&D expenditure data for instance, specific technologies individually do not appear in the main sections of the major statistics offices, thus it is difficult to aggregate. The overall level of technology is not being measured and displayed either. Trade statistics in connection with technologies, or the level of technology are similarly hard to find. One data collection both the World Bank (see Figure 3) and Eurostat look at though, is high-technology exports.

Figure 3. *High-technology Exports (% of Manufactured Exports)*

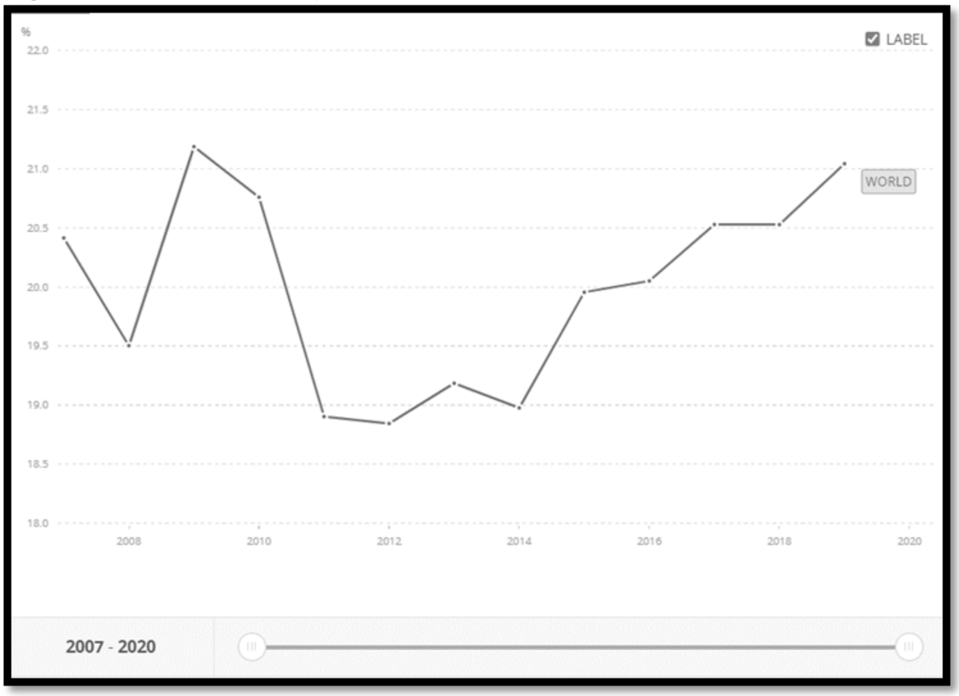

Source: The World Bank (2021).

The problem with such statistics is that the definition of "high-technology" is rather vague: "High-technology exports are products with high R&D intensity, such as in aerospace, computers, pharmaceuticals, scientific instruments, and electrical machinery" (The World Bank 2022). It is not guaranteed that technology level movements in time are reflected too, overall, in such data.

Technology levels related concepts described in articles on trade dynamics include phenomena partially touched upon in the subchapter on endogenous growth: technology leaders and followers, knowledge diffusion, and the technology gap. The actors and processes behind these concepts may yet be different from what the reader might expect. In the article *Human Capital and Technological Catch-Up of Developing Countries: In Search of a Technology Leader*, which used the so-called Nelson-Phelps model to revisit technological diffusion and catch-up, it is stated how a group of countries (the OECD and regional leaders, in this case) serve better as technology leaders for developing countries, than having that role designated to one single, (geographically relatively distant) state, namely the US (AtiqurRahman and Zaman 2016, p. 168). The "extent of […] technology in the export structure" (McAuthur and Sachs 2002, p. 43) is another term linking technology levels with trade dynamics.

Indicators

Moving slightly closer to concepts and indicators of direct use when aiming for measuring the level of technolgy, it is worth looking at the state of science, technology and innovation (STI) indicators, measured by various international organisations. These indicators show GDP proportionate expenditures on research and development (R&D), by country and region. The OECD's STI Scoreboard provides such an opportunity, (OECD 2022a) along with an outlook document (OECD 2022b) and a site (OECD 2022c) for related policies. The United Nations Conference on Trade and Development (UNCTAD) has a detailed methodology for STI measurement, for the firm level, in the public sector, and at the system level too (UNCTAD 2010, p. 3).

These indicators may provide more spectacular information, especially in terms of comparisons, than the World Bank data did, in the context of the present paper. Yet, for economic theory in general, there is still a lack of absoluteness regarding the level of technology.

Frontiers

Another step closer to measuring technology levels is identifying its main frontiers. Prior to mentioning concrete frontiers[8], however, it should be noted that human needs (e.g., employee needs) have started to emerge in competitiveness and technology reports, (World Economic Forum 2020, p. 6), such as the World Economic Forum's *2020 Global Competitiveness Report*, which identifies technology as a response tool (World Economic Forum 2020, pp. 47, 55). The role of human needs in measuring the level of technology will be reemphasised and explained in the next main chapter of this paper.

[8]As for frontiers, the frontier of technology should in no case be confused with the production possibility frontier.

Frontier technologies as classified by the UNCTAD *Technology and Innovation Report 2021* are as follows: Artificial Intelligence (AI), Internet of Things (IoT), Big data, Blockchain, 5G, 3D printing, Robotics, Drone, Gene editing, Nanotechnology, Solar photovoltaic (UNCTAD 2021, p. xvi).

Particularly interesting from the economic perspective will be to observe how one of the above frontiers, namely AI, will become more interwoven with economics. Questions may arise, such as: Do individuals know best what they actually need? How long would mainstream models of the economy be applicable? Would the applicability change with individuals relying more and more on, and accepting AI algorithms and smart devices telling them what they need?

The disruptive frontier technologies may not just influence or change the economy, they may alter and assist sciences as well. For instance, AI may assist economics in shifting further away from the homogeneous homo oeconomicus model, through patterns and categories of agent diversification.

The importance of human needs has already been indicated. At this point, AI as a frontier, needs, and knowledge can be connected, as for many of the individual problems, solutions exist in the initial form of knowledge. Knowledge is spreading and sticking fastest and strongest along needs. And likely candidates for recognising individual needs on a larger scale are artificial intelligence programmes.

Jumping slightly ahead, through moral economics, AI can be put into the bigger economic picture as well, through its own potential morality. However, most of those familiar with the concept of supermoral singularity seem to be afraid of it. Presumptions generally omit the possibility of humans possessing undiscovered virtues. The chance for societies having intrinsic, genious-by-design mechanisms is also left unregarded.

The Gap of Concrete Measurement

As it was presented in the sections above, there are several approaches to, and uses of the level of technology, but there is a lack of punctuality, theoretical usefulness and absoluteness. Similar as for utility, for the level of technology too, economists would need a scientific measure, a more concrete construct.

The gap appears in works as significant as Thomas Piketty's *Capital in the Twenty-First Century*: "[…] β was fixed by the available technology […] so that the growth rate was entirely determined by the savings rate" (Piketty 2014, p. 230). The concept of available technology (the given level of technology), however, is not being further elaborated on, or quantified for the fix mentioned.

Despite being unanswered, the question or gap of measurement is not novel. In a 1969 article on technological change, William Nordhaus identified the "absence of an adequate theory" that would explain the part of growth of output, which the growth of input in time could not. Nordhaus was seeking answers through his microtheory of the generation and transmission of new knowledge, (Nordhaus 1969, p. 18) but the ultimate goal of measuring the technology levels has not been stated. Nordhaus was focusing on the causes of change, but not the levels themselves: "Although technology has long been recognized as an important part of the economic scene, invention has not been fully integrated into economic analysis. (Invention will be used as a general term for activities which expand the level of technical knowledge)" (Nordhaus 1969, p. 18). This paper suggests a different approach.

It appears that the traditional branch of economics alone is less able (or its representatives are less willing) to provide a scale for unified technology measurement. Thus far, the factor *along* which the level of technology is to be measured, has not been fixed – which is where moral economics and human needs come into the picture.

Measuring the Level of Technology in Moral Economics

Thus far, the reader could familiarise themselves with a geographically and temporally rich and beneficial base of technology level applications. The research will now narrow the focus, and zoom in on the theoretical and technical details.

As a matter of fact, there have been no successful attempts for an absolute quantification of technology levels. Thus, economics in regard of technology is lacking: methods of measurement; designated starting- and end points; milestones; and a unit of measure.

Moral economics – the branch that aims at incorporating the ethical factor into economic models – may have an advantage here, for two reasons: (1) It does not abstain from normativity. (2) It gives space for human needs to play a central role.

These statements will be elaborated in the subchapters to follow, thus let it now suffice to briefly connect the two statements by saying: If satisfying needs is a natural instinct or aspiration, then human progress should not be judged unnatural overall.

Compatible Axioms

The scarcity premise of the classical/neoclassical school points to a model with people's needs being infinite and insatiable. In moral economics, however, human needs are ultimately finite and satiable (which is one of its adjusted axioms) (Hajnal 2020, p. 66). Humans are the main drivers, carriers and beneficiaries of technology, and they also hold the key to measuring its level, through their needs. "Marrying" needs as a factor, and the level of technology, is carrying the potential of redefining technology, taylored to the human needs concept.

In a recent doctoral dissertation, looking into innovation theory, it has been suggested that the next Kondratiew-waves will have – in contrast to the earlier themes of machines – the human person in their focus, potentially expanding this new viewpoint onto the entire planet. After the – also: pandemic-induced – motto "heal the human", the next, "heal the planet" will gain centre stage (Stukovszky 2022, p. 25). This is a modern view, which resonates well with alternative branches of economics, such as Buddhist economics, and moral economics as well.

As for the normativity theme, in the current context one may ask if the level of technology should draw any normative (value) judgement upon itself? From the general starting point of the whole economic system, in practice, it could not be avoided. Changing levels of technological progress historically tailor positive and negative implications, on the different stages. The subject of technological dualities has been touched upon, for instance, in Martin Heidegger's widely known book, *The Question Concerning Technology* (Heidegger 1954, pp. 83, 105). Moreover, certain technologies are seen as inherently violent, "brute force" technologies (Josephson 2002), in contrast to inherently non-violent ones.

The latter statements, however, do not suggest that technology (and its increasing levels) would be a comprehensive cure for societal issues in itself. "Progress toward economic and technological rationality need not imply progress toward democratic and meritocratic rationality. […] technology, like the market, has neither limits nor morality. The evolution of technology has certainly increased the need for human skills and competence. But it has also increased the need for buildings, homes, offices, equipment of all kinds, patents, and so on, so that in the end the total value of all these forms of nonhuman capital (real estate, business capital, industrial capital, financial capital) has increased almost as rapidly as total income from labor. If one truly wishes to found a more just and rational social order based on common utility, it is not enough to count on the caprices of technology" (Piketty 2014, p. 234). Technology in itself is necessary, but – despite the gain on normativity one achieves by modifying technology levels' definitions – not sufficient.

"Stock" vs "Flow" Nature, Supply- vs Demand-Side Measurement

Overall and in general, there are essentially two ways to look at technology in the context of human progress. One can view the process of technological advancement more as a path (a "flow") that humankind is on. The other way to look at it is in terms of accumulation.

The "flow" perspective is overrepresented as the general modern viewpoint, yet there are economists, who touched upon, or even delved into the accumulative nature of technological progress, such as the late Hungarian economist and engineer Ferenc Jánossy, with his trendline theory (Bekker 1995).

The overrepresented "flow" nature results in the dominance of relative measuring, as opposed to absolute scales and numbers, for which the "stock" nature provides enough space and methods. Instead of measuring just technological change (as in a flow), moral economics too has the ambition to attempt measuring the level of technology as an absolute value, in the process of progress.

Measuring the level of technology can also be classified in supply- and demand-side approaches. As per Perilla Jimenez: "there is a striking amount of dimensions in which the innovation issue can be analyzed, including both supply and demand sides of the economy" (Perilla Jimenez 2019, p. 829). What is meant in this paper by supply-side measurement is a focus on productivity and effectiveness through engineering parameters dominating the scales, which is well illustrated, for instance, by Moore's law, and microprocessor performance chronology (Aizcorbe and Kortum 2005). This "technolgy-for-the-sake-of-technology" type of attitude is the more widespread approach of the two, and results from the economic practice of relating "technology to "something' that increases productive efficiency, offsetting the tendency of other factors (capital, labor) to yield decreasing returns" (Perilla Jimenez 2019, p. 826).

On the other hand, there is demand-side measurement, envisioned within the field of moral economics. It refers to the level of technology being defined by its function and capability of satisfying human needs[9] and fostering human progress. Measuring the level of technology in moral economics (from the demand side) may be judged as more utilitarian than the traditional measurment method.

If the level of technology were to be defined by the demand side, it could not avoid a historical element. It can be put as follows: The extent to which the scientific knowledge of the time can optimally be applied to satisfy human needs.[10]

The intriguing point is that moral economics uses a finite and satiable axiom of human needs, thus it would allow for a steady-state-technology, or an end-of-technology, if human needs were to be satisfied fully and sustainably. (More on this in the subsequent subchapters.)

Moreover, a demand-driven definition of technology levels would alter the definition of technology itself, not necessarily by changing the wording, but by having transformed it into a normative concept, with expressedly human end goals. One should note, however, that taking, for instance, Heidegger's lines – about how the technical concerns the revealing of truth (Heidegger 1954, pp. 106, 108) – into account, the distancing of the meaning of technology from the technical in itself is not completely new in social science. It aligns with the "embodiment notion" in its process, yet contrasts with it in technology not being something "that is primarily embodied in artifacts" (Perilla Jimenez 2019, p. 826).

Historical and Geometrical Methods of Constructing Scales, and the Steady-State-Technology

As a last dimension of technology level measurement classification, historical and geometrical methods will be presented here.

As for the historical method, the expectation with this approach is that discovery and innovation milestones be determined, from both the human need related, and the technical perspective. In the literature on innovation theory and technology cycles[11] there is generally not a word mentioned on ultimate technology directions or goals, for the ambitiousness of the endeavour to determine them.

According to the moral economic approach, technology may have a minimum or start, and a maximum or end. The start is difficult to define, the end is difficult

[9]Perilla Jimenez refers to technology as being "forged through the organization, functioning, and needs of the society at large" (Perilla Jimenez 2019, p. 826, footnote 8).
[10]A more inclusive and holistic definition (relatable to Buddhist economics) would refer to the needs of all living beings.
[11]See, for instance: Szanyi (2021).

even to imagine, so the paper will stay hypothetical on this topic. The start is proposed to be determined by the first human invention, or the first human imitation of nature. Without details on the significance of individual inventions – which is out of scope and capacity for this paper – the method jumps to determining an end-point.

The end could be the so-called steady-state technology. (If the level of technology reaches its "top", it does not mean that the economy too has to be steady-state, that is, the lack of further developments would not hinder economic expansion, i.e., growth.) This steady-state end-of-technology would be characterized by an absolute well-being (fully and sustainably satisfied human needs, and ideally of all living beings). If it were not just needs under consideration as conditions, maximal effectiveness and sustainability of processes, and the completion of the body of knowledge could be added – all unprecedented, yet theoretically existing objectives.

After designating the two ends of the technological scale, the unit of measure and the current position are to be determined. This is the point where the geometrical method completes the picture. The geometrical measurement of the level of technology generally means functions "drawing closer" to the vertical axis in their respective economic models: in neoclassical, as well as in moral economic ones.

In the neoclassical sense, this is what was illustrated with the microeconomic production function. As for moral economics, the author takes a model (illustrated in Figure 4), where the hypothetical aggregate of human needs and potential output are depicted (measured on the vertical axis) as a function of the population number (horizontal axis):

Figure 4. *Human Needs and Potential Output*

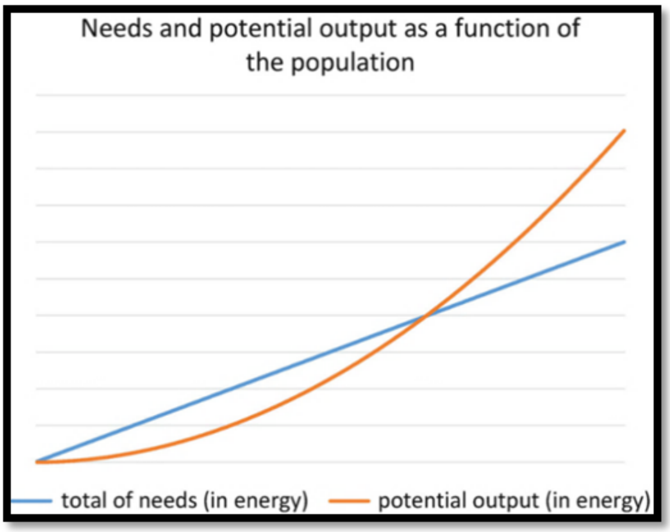

Source: Hajnal (2020, p. 78).

With time, technological progress draws the upward bending "potential output" function closer to the Y axis, as depicted in Figure 5. The closer it is, the more technologically advanced a society, as there are fewer people needed to produce the same amount of output. The aggregate needs function, however, remains static:

Figure 5. *Different Levels of Technology*

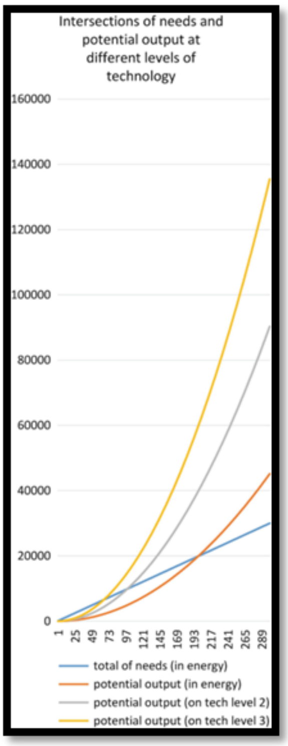

Source: Hajnal (2020, p. 85).

Over a certain level, technological advance is self-perpetuating. "Each new technological innovation triggers yet further innovation, in a kind of chain reaction that fuels long-term economic growth" (McArthur and Sachs 2002, p. 29). According to this observation and logic, the positive changes in "potential output", as on the graphs above, can be expected to occur at an ever increasing pace. The acceleration is justified not just by chains, linear processes as outlined above, but also by network effects. New forms and actors of technology and – more specifically – "innovation do not emerge independently […]; rather, they are interconnected with each other" (Hámori and Szabó 2016, p. 52).

The steady-state of technology would be the output function becoming fully vertical, that is, people not needing to work anymore themselves, whilst remaining capable of satisfying their needs. In the geometrical approach to technology level measurement, it is rather the minimum level of technology that is difficult to determine. Where is the function the "flattest"? How did it start "bending up"? It must have been nature to give us the starting push, but how exactly? These questions would push the paper into the realm of evolution and cognitive science, which currently – again – is out of scope. Independently of these questions, once the factors are quantified, the level of technology can be measured along the tangential lines (to the output functions).

The moral economic view of technology levels has an allegory, in the "mountain of progress" (Hajnal 2015, p. 34). The levels of technology can be imagined as different stages on this mountain. Each stage is a step in human life getting better in general, moreover, the individual levels of well-being are determined by this overall level too. There are steps of different sizes, depending on the significance of progress made in satisfying a given human need with a given new technology. Through counting the (weighted) steps from the "start", and estimating them to the "top", it is possible to determine the current level on the path, up that mountain, which is the allegoric version of combining the presented historical and geometrical methods. This version is a broad interpretation though.

Finally, it should be emphasized that in practice, technology is just one pillar of human progress. As another pillar, the quality of public institutions (McAuthur and Sachs 2002, p. 45) could be named.

Conclusion and Outlook

Throughout this paper, various approaches, applications and methods of measuring the level of technology have been looked into. It started with the micro- and macro-economic models, which, even if carefully selected, according to relevance, barely touch upon the subject of technology levels. In trade models, statistics and dynamics, the level of technology gains on importance, yet is rarely expressed explicitly. Through indicators and frontiers, one is equipped with more tools, still far from a concrete and unified theory or method though.

Moral economics has been brought into the picture, because through its axiom of finite and satiable human needs, this economic school carries the potential of defining technology through its capability of satisfying those needs, ultimately constructing a finite scale for technology levels. In order to describe economies more and more comprehensively, with the advance of the economic fields of science, accurate technology level measurements are unimaginable to bypass. On the quest for the "holy grail" of economics, or an economic "theory of everything", but even in the more modest economic endeavours, the level of technology must be a part of the equations. This measure should be "precise enough to represent trends in specific countries yet broad enough to allow global comparability is a long-term research endeavor" (McAuthur and Sachs 2002, p. 39). The level of technology, if applied in the form as it was approached in this paper, should be applicable to both to technoligical "leaders", and the pace of their innovative journey, as well as to their "followers", signalling their speed of absorption and implementation.

The paper has opened a door to an alternative way of measuring the level of technology. Accepting and refining the moral economic measurement method could result in a reinterpretation of technology overall, casting a novel viewpoint on future technologies. Special attention should be brought to the theoretical end point it enables. The circumstances of this "steady-state technology" may yet be unimaginable, but the conditions can be set, if one ties technology to needs.

Acknowledgments

The author is grateful to her supervisor, Dr. Balázs Hámori, for his critical review and thoughtful comments.

References

Aizcorbe A, Kortum S (2005) Moore's law and the semiconductor industry: a vintage model. *The Scandinavian Journal of Economics* 107(4): 603–630.

AtiqurRahman AKM, Zaman M (2016) Human capital and technology catch-up of developing countries: in search of a technological leader. *The Journal of Developing Areas* 50(1): 157–174.

Bekker Z (1995) On Jánossy's trendline at the end of century, or, can we get rid of our past? *Acta Oeconomica* 47(1/2): 95–109.

Encyclopedia Britannica (2021) *Technology*. Encyclopedia Britannica. Retrieved from: https://www.britannica.com/technology/technology. [Accessed 14 February 2022]

Hajnal Z (2015) Írott és íratlan értékek az ENSZ Alapokmányának Preambulumában – Az emberi együttélés és haladás axiómái. (Written and unwritten values in the preamble of the United Nations charter – The axioms of human coexistence and progress). *GROTIUS* e-journal, Corvinus University of Budapest. Retrieved from: http://www.grotius.hu/publ/displ.asp?id=MOMPOO. [Accessed 10 January 2022]

Hajnal Z (2020) *Moral economics - A theoretical basis for building the next economic system*. In *Words, Objects and Events in Economics - The Making of Economic Theory*. Springer.

Hámori B, Szabó K (2016) *Reinventing innovation.* In M Rosta, B Hámori (eds.), *Constraints and driving forces in economic systems: studies in honour of János Kornai.* Newcastle upon Tyne, United Kigdom: Cambridge Scholars Publishing.

Heidegger M (1954) *Die Frage nach der Technik.* (The question concerning technology). Retrieved from: https://www.bard.edu/library/arendt/pdfs/Heidegger-Frage.pdf. [Accessed 15 February 2022]

Josephson PR (2002) *Industrialized nature: brute force technology and the transformation of the natural world.* Washington: Shearwater Books.

McAuthur J, Sachs JD (2002) *The growth competitiveness index: measuring technological advancement and the stages of development*. Center for International Development at Harvard University

Nordhaus WD (1969) an economic theory of technological change. *The American Economic Review* 59(2): 18–28.

OECD (2022a) *Science, technology and innovation scoreboard*. Retrieved from: https://www.oecd.org/sti/scoreboard.htm. [Accessed 9 January 2022].

OECD (2022b) *Science, technology and innovation outlook*. Retrieved from: https://www.oecd.org/sti/science-technology-innovation-outlook/. [Accessed 9 January 2022]

OECD (2022c) *STIP compass*. Retrieved from: https://stip.oecd.org/stip/. [Accessed 9 January 2022]

Perilla Jimenez JR (2019) Mainstream and evolutionary views of technology, economic growth and catching up. *Journal of Evolutionary Economics* 29(Feb): 823–852.

Piketty T (2014) *Capital in the twenty-first century*. Cambridge, Massachusetts: The Belknap Press of Harvard University Press.

Romer PM (1994) The origins of endogenous growth. *The Journal of Economic Perspectives* 8(1): 3–22.

Samuelson PA, Nordhaus WD (2010) *Economics*. Nineteenth Edition. New York: McGRAW - HILL.

Seo SN (2017) 5 - Breakthrough technologies: technological innovations as an alternative global warming solution. In *The Behavioral Economics of Climate Change*, Academic, 139–183.

Stukovszky T (2022) *Az innováció alakulása válság idején a 21. századi EU járműiparában.* (Innovation in the 21st century EU automotive industry in times of crisis.) PhD Dissertation. Corvinus University of Budapest, Doctoral School of International Relations and Political Science, Department of World Economy.

Szanyi (2021) Catching-up opportunities of East-Central European states in the context of technology cycles. In T Gerőcs, J Ricz (eds.), *The Post-Crisis Developmental State*. International Political Economy Series. Palgrave Macmillan, Cham.

The World Bank (2021) *High-technology exports (% of manufactured exports).* Retrieved from: https://data.worldbank.org/indicator/TX.VAL.TECH.MF.ZS. [Accessed 5 December 2021]

The World Bank (2022) *High-technology exports (% of manufactured exports).* Retrieved from: https://tcdata360.worldbank.org/indicators/mnfc.TX.VAL.TECH.MF.ZS?country=BRA&indicator=2010&viz=line_chart&years=1988,2019. [Accessed 9 January 2022]

Trefler D (1995) The case of the missing trade and other mysteries. *The American Economic Review* 85(5): 1029–1046.

UNCTAD (2010) *Science, technology and innovation indicators for policymaking in developing countries: an overview of experiences and lessons learned* Retrieved from: https://unctad.org/system/files/official-document/ciimem1crp1_en.pdf. [Accessed 9 January 2022]

UNCTAD (2021) *Technology and innovation report 2021*. Retrieved from: https://unctad.org/webflyer/technology-and-innovation-report-2021. [Accessed 5 December 2021]

Veiseh N (2010) Reconciling Acemoglu and Sachs: geography, institutions and technology. *Journal of International Affairs* 64(1): 205–220.

World Economic Forum (2020, December 16) *Global competitiveness report special edition 2020: how countries are performing on the road to recovery.* Retrieved from: https://www.weforum.org/reports/the-global-competitiveness-report-2020. [Accessed 5 December 2021]